RESPONSE BY THE AUTHOR

First of all, than you for your comments! They were of great help in improving this study. I first reply on some major comments you both had and then, I reply to each of the comments separately.

1 MAJOR CHANGES AND RESPONSE TO COMMON COMMENTS

1.1 SHORTENING THE MANUSCRIPT

We analyzed a long data set in this study and we presented a lot of figures in the first manuscript. To emphasize the important parts of the manuscript, such as the trend analysis and RFE, we removed some of the figures as you recommended. For example, we got rid of the PM1 panels on some of the figures, since they gave no extra information that was relevant for this study. We also removed the section about the new particle formation events and aerosol optical properties. We agreed that it did not fit in the topic of this manuscript. I moved the old Fig. 3 to the supplementary material, since it was referred only once in the text. I moved the old Sect. 3.5 (Diurnal variation) to the supplementary material. The diurnal variation was a bit separate from the rest of the manuscript and it did not present any new information to Virkkula et al. (2011). I also moved the old Fig. 11 to the supplementary since after adding the seasonality and ambient RH to the RFE analysis, this figure did not feel important anymore. The number of figures decreased from 12 to 8 and the number of subfigures decreased as well. However, the supplementary material grew from one figure to nine figures since we answered to some of your questions without increasing the number of figures in the main article.

Since we added more description in the method section and improved the discussion we got now more text. We also added one table, which describes how the trend varies between different seasons.

1.2 SIZE DISTRIBUTION ANALYSIS

We are still keeping the size distribution analysis, since we found it interesting to study how the aerosol optical properties and their trends are related to the size distribution. For example, in Pandolfi et al., (2018) they were not using size distribution data and they had to assume what kind of changes in the size distributions cause the different types of trends for the α_{sca} observed at different stations. The study on the size distribution helps us to understand how the size dependent b and α_{sca} vary between PM1 and PM10 measurements. However, we moved part of the size distribution analysis (old Fig. 3) to the supplementary material.

1.3 CALCULATION OF RFE

Another thing you both pointed out was the calculation of RFE by using global average values. We worked more with the topic and determined a more realistic RFE at SMEAR II. What I found difficult was determining the b for moist conditions and I had to make rather rough estimates there. This would be an interesting topic to study more.

To emphasize the meaning of RFE: as stated by Sherman et al. (2015), the RFE ($\Delta F\ \delta^{-1}$) provides a means for comparing the intrinsic forcing efficiency of aerosols measured at different sites. The RFE describes the change that aerosol particles would have on the top-of-atmosphere radiative forcing (ΔF) per unit of aerosol optical

depth (δ). Since AOD is unitless, the unit of RFE is W/m2. The RFE is an intensive property and it does not depend on the amount of aerosols. If we wanted to know the Δ*F*, we would need measurements of δ, which, on the contrary, is an extensive property and depended on the amount of aerosols.

We have now determined three different types of RFE values:

1) $RFE_{H\&S}$ was calculated by using the constant values suggested by Haywood and Shine (1995). $RFE_{H\&S}$ was derived for dry particles. Here the subscript "H&S" refers to Haywood and Shine (1995).

2) RFE_S was calculated by using seasonal averages for the environmental parameters (D, A_C, R_S). So here we let the fractional day length to vary; we used more realistic values for the surface reflectance according to Kuusinen et al., (2012) and took the snow cover into account; and we determined an average cloud fraction for each month. More detailed description is provided in the manuscript in Sect. 2.3.3 (p. 8 – 10). We added a figure in the supplementary material (Fig. S1a-c) describing the seasonal variability of these parameters. RFE_S was derived for dry particles. Here the subscript "S" refers to "seasonal".

3) $RFE_{S,moist}$ was calculated similarly to RFE_S, but taking the ambient RH into account. Here we determined average RH for each month and we derived the AOPs to the average humidity. The seasonality of RH is presented in Fig. S1d. In determining the ω_0 for humid conditions, we assumed that the absorption does not depend on the RH. The scattering was converted to humid conditions using the parametrization provided by Zieger et al. (2015), which is presented in Sect. 2.3.1. The parametrization was given only for total scattering so we could not use it for backscattering and determine b with this parametrization. Instead we assumed that the b has a linear dependency on RH. Fierz-Schmidhauser et al. (2010) observed that the b decreased 30 % when the RH increased from dry conditions to 85 %, which we used in this study. Here the subscript "S,moist" refers to "seasonal" and ambient RH, which was > 50 % for each month. This is described in Sect. 2.3.3 (p. 10).

The results for different RFE values are presented in Sect. 3.6, Table 1., and Fig. 7.

1.4 DATA PROCESSING

You both commented that I should apply the truncation correction also to backscattering data. This has now been done.

I also made a small change to the Aethalometer flow correction (Fig. S2 added in the supplement), and changed the C_{ref} value from 3.35 to 3.19. Thus there are small changes (less than 5 %) in the data presented in the article.

In this new version of the manuscript we have discussion about how the RH affects the scattering. Therefore we present the parametrization of the scattering enhancement factor in the Sect. 2.3.1. I have also added a better description about the Aethalometer correction algorithm used here. Since we were not able to submit my second manuscript, which would have presented the C_{ref} at SMERA II, I added a short description about C_{ref}.

2 RESPONSE TO MAJOR AND SPECIFIC COMMENTS

The comments by the referees are listed with bolded font and the response by the authors are written with normal font. If the answer refers to a text that was added in the manuscript, the quotation is italicized.

2.1 REFEREE 1

GENERAL COMMENT

The here presented manuscript describes the variability of several aerosol optical properties (AOPs) measured in southern Finland for more than a decade. The multi-year variation of AOPs is presented together with a detailed analysis of AOPs variability on a shorter timescale. Due to its time coverage, the dataset presented here is of great relevance and might help to understand how aerosol changed in a North European background site during the last ten years. The scheme and structure of the manuscript are linear and follows a logical order. However, the amplitude of the dataset generates a certain overloading of the manuscript, meaning that the results are not always properly discussed within a climatologic perspective but simply described. As a consequence, is difficult to identify the overall scientific message of the work. I truly believe that the paper covers the topic of interest of ACP, but I would recommend the authors to improve the discussion and interpretation of their results in order to better transmits their message to the readers. Hopefully, the major and specific comments reported below will help the authors to improve their work.

We have now worked with the manuscript and improved the discussion especially in the sections that concern trend and RFE. We have also decreased the number figures in order to make the manuscript more readable and less crowded.

MAJOR COMMENTS

I have the strong feeling that the manuscript is overloaded with figures, especially multipanels figures. First of all, due to the similarity between PM1 and PM10 (Figure 1, 2, 4), the discussion and presentation of results become particularly redundant in Section 3.2, 3.3, 3.4. The subsequent effect is that the discussion often focusses on the differences between the two aerosol fractions rather than on the reasons leading to the multi-year trends or seasonality. I thus suggest the authors show and describe PM10. This will lighten the paper and give more space for the climatologic interpretation of the results. Moreover, it appears that a considerable number of figures is poorly described or is not essential to the understanding of the results. I thus suggest the authors to reconsider the absolute relevance of certain graphs and to remove them from the manuscript or move them to the supplementary. More details can be found in the specific comments.

I have now modified the multipanel figures so that they include only PM10 data, if the PM1 data presented no additional information. Some of the figures, which did not seem that relevant anymore, I have moved to the supplementary material.

The dataset allows the investigation of multi-year variability and trends of AOPs and size distribution. The variability of AOPs is also investigated on a shorter time resolution but ignoring the year-to-year variability (Section 3.4, 3.5, 3.6). Thanks to the long-term measurement I would expect a work focusing on trends and multiple-year variability of AOPs. However, the analysis of trends is disconnected from the seasonal and diurnal variability and the consequent RFE. Therefore, I have some troubles in understanding what is the topic or scientific question acting as a glue between the sections, which in some cases (Section 3.3.1, 3.5 and 3.6) appear to be self-standing. I would thus suggest the authors to better exploit their long time series and focus on the long-term evolution/variability of AOPs including trends, impacts on seasons and, potentially, diurnal

variability. For instance, Section 3.3.1 is based on 2 months measurements only, what is the long-term implications of NPF on the aerosol optical properties, and is this short period representative of the 10 considered years? Moreover, Section 3.5 provides the diurnal variability of AOPs. Despite the fact of a weak variability, was the boundary layer dynamic changing within the 10-year period? It is hard to understand the relevance and implications of such variability. Similar reasoning applies to the monthly variability, did summer and winter experienced a change from 2006 to now?

There is now a figure in the supplementary material (Fig. S3) that better describes the year-to-year variability of scattering, absorption and particulate volume for each season. The figure presents the time series of monthly medians separately for each season. It can be seen from the figure that the year-to-year variability is the highest in winter, when the amount of pollution is highly depended on the meteorological conditions, which is discussed in the supplementary.

To connect the trend analysis to the seasonal variation we determined trends separately for each season. The results are presented in Table 4 of the manuscript.

I agree with the Sections 3.3.1 and 3.5 being self-standing and we chose to remove 3.3.1 from this manuscript. Sect. 3.5 I chose to move in the supplementary.

The calculation of the forcing efficiency is an extremely interesting topic, and up to me a decadal trend of RFE might represent the core of the entire manuscript together with Section 3.2 and 3.3. However, for the RFE estimations, the authors assumed the atmospheric (RH, cloud) and environmental (surface albedo, day length) variables as constant, which are not even specific for the SMEAR II station. Due to strong seasonality and, potentially, year-to-year variability of such variables, the final RFE estimations are unrealistic. I would suggest the authors implement constants representative, at least, of Southern Finland or, better, to use seasonal dependent variables. Other than that, any conclusion on climatic impacts of aerosol at SMEAR II will be highly questionable and of low interest.

We have now worked more with this topic. See my answer 1.3 in the beginning of this document.

SPESIFIC COMMENTS

P3L11: Why MAAP and PSAP are introduced if only data from the AE31 are used?

I removed PSAP from the introduction but I left MAAP since I added a short description about the multiple scattering correction factor (C_{ref}) (see my response to comment about P3L23), which was determined by comparing Aethalometer and MAAP measurements.

P3L13: This is irrelevant for the present manuscript.

I removed this sentence.

P3L23: I would say that, since Luoma et al. 20xx is not available, a better description should be provided here.

I removed the self-citation from the manuscript. We had too optimistic expectations about the timetable with the other manuscript. We hope to submit the manuscript by the end of this year. I have also added a better description about determining the C_{ref}:

"The C_{ref} was determined by comparing the Aethalometer data, that was corrected only for the filter loading artefact, against the reference absorption coefficient ($\sigma_{abs,ref}$) measured by the MAAP.

$$C_{ref} = \frac{\sigma_{ATN}}{L \cdot \sigma_{abs,ref}}. \quad (6)$$

The resulted median value for C_{ref} was 3.19, with a standard deviation of 0.67. "

P3L31: Can the author exclude the influence of hygroscopic growth?

When the particles enter the electric charger, the sample air is not dried. However, since the sheath air is dried, the aerosol particles are also dry in the DMA of the DMPS setup. I added this explanation to the manuscript:

"There is no active drying system in the TDMPS sample line to prevent particle losses. However, the sheath flows, which are used in the TDMPS system, are dried (RH < 40 %) so the particles are sampled in dry conditions."

P4L4: Which instruments, all of them?

I meant only instruments that measure optical properties. For other instruments we should not have this problem. I fixed the sentence to:

"In the present work, if the internal RH in any of the optical instruments exceeded 40 %, the data from that instrument were excluded from further analysis if not stated otherwise."

P4L11: It is not clear why the truncation correction was not applied for the backscattering. Does it mean that back-scattering can be affected by systematic error compared to total scattering? Was this assessed? Was it negligible? The authors present more than 10 years of data, more care in the presentation of the data correction is mandatory.

Now, also the backscattering is corrected.

P4L19: Multiple correction procedures were used or only the Collaud Coen et al. (2010) as stated later? If the correction of Collaud Coen was used, I honestly do not see the reason to cite all the other algorithms. Generally, I would not recommend the frequent self-citation of works that are not ready yet.

I removed the self-citation and the citations to the other correction algorithms that were not used here. I added a description of the correction algorithm in the text:

"Here, we corrected the Aethalometer data by using the correction algorithm described by Collaud Coen et al. (2010)

$$\sigma_{abs,i} = \frac{\sigma_{ATN,i} - a_{s,i}\bar{\sigma}_{sca,s,i}}{C_{ref}\, L_{s,i}}, \quad (3)$$

where

$$L_{s,i} = \left(\frac{1}{l(1-\bar{\omega}_{0,s,i})+1} - 1\right) \cdot \frac{ATN_i}{50\ \%} + 1, \quad (4)$$

and

$$a_{s,i} = \bar{\zeta}_{sca,s,i}^{d-1} \cdot c \cdot \lambda^{-\bar{\alpha}_{sca,s,i}\cdot(d-1)}. \quad (5)$$

In Eqs. 3 and 4, the subscript i indicates the number of the measurement and the subscript s indicates the average properties of the aerosol particles that are embedded in the filter spot. The over lined parameters are mean values from the start of the filter spot to the ith measurement. In Eq. 3, the σ_{ATN} is the attenuation coefficient reported by the Aethalometer, a is the scattering correction parameter, C_{ref} is the multiple scattering correction factor, and L is the loading correction function. In Eq. 4, the ω_o is the single scattering albedo (see Sect. 2.3.3) and the ATN is the light attenuation through the filter spot in percentages. In Eq. 5 the ζ_{sca} is the proportionality constant of the wavelength power law dependence of σ_{sca} and α_{sca} is the Ångström exponent of the σ_{sca} (see Sect. 2.3.3). For l, d, and c we used values 0.74, 0.564 and 0.329 $\cdot 10^{-3}$ respectively. For scattering correction, we used measured σ_{sca} values that were interpolated and extrapolated to the AE-31 wavelengths. Note that most of the symbols used for the variables are different from Collaud Coen et al. (2010). The reason is that in the present work the symbols are used for other variables below."

P6L15: I expect that BC from biomass burning and traffic has a different chemical composition. Isn't it in contrast with lines 13-15? If α_{abs} is simultaneously affected by size, chemical composition, sources and mixing, to what purpose is α_{abs} used here?

I guess the Aethalometer model assumes that the α_{abs} is only depended on the chemical composition, which then depends on the source. In Hyytiälä, the BC particles are typically aged so they probably have a coating that affects the α_{abs} and because of this the Aethalometer model might not be functioning in Hyytiälä. We added some discussion about the aethalometer model in the discussion section:

"Also, the α_{abs} is typically associated with the source of the BC and it is often used to quantify whether the BC is traffic or wood burning related (Sandradewi et al., 2008; Zotter et al., 2017) so that high α_{abs} is a sign of wood burning. In the source apportionment, α_{abs} close to one indicates that the BC is sourced from traffic. Since we observed relatively higher α_{abs} in winter, the results are in line with the assumption of domestic wood burning that takes place during winter. However, in summer, α_{abs} was often < 1, which would yield an unphysical fraction (over a 100 %) of traffic related BC. Values below 1 could have been caused by large BC particles (D_p > 100 nm) that have a purely scattering coating (Lack and Cappa, 2010). It must be noted that the α_{abs} depends also on the correction algorithm. For example, if the σ_{abs} was corrected with the algorithm proposed by Arnott et al. (2005), the mean ± SD of α_{abs} would have been 1.36 ± 0.51 (see Table S2). Using the α_{abs}, which was determined by using the correction by Arnott et al. (2005), the results for the source apportionment would be different and they would show higher fraction of BC from wood burning. Further investigation of the complex nature of α_{abs} is omitted here."

P6L22: Equation 5 is quite different from Haywood and Shine (1995), is this the original source of the equation? What is the wavelength of RFE? Is then the aerosol optical depth measured or everything is calculated from Equation 5? Though I have quite some doubts on the choices of constants (see comments on Section 3.7), a better description of the equations and its limits should be provided, together with the motivations at the base of the choices of the constants and the subsequent uncertainties.

It is the same equation as the Eq. 3 in Haywood & Shine (1995) but divided by the AOP. This was derived by Sheridan and Ogren (1999) (Eq. 8), to which I was missing a citation. Here we have not used the measurements of AOD. Haywood & Shine used the constants for calculating the ΔF independent of wavelength and Sheridan and Ogren (1999) used these same values in calculating the RFE at 550 nm. In addition to the H&S constants, we now calculated the RFE by using seasonally varying environmental parameters (see my 1.3 at the beginning of this document). Using seasonally varying parameters give some estimate about how realistic the RFE calculated by using the constant values is.

P10L5-17: This part of the section mostly describes the technical aspects of the measurements. I would suggest to move them in the method section. Potentially into a new subsection discussing the data coverage and how the data set was reduced/validated.

I moved this part to a new section "2.3.4 Data coverage" and described the data coverage better. I also added a table in the supplementary material where the data coverage from each month is presented.

"If averaged over the whole measurement period, 81 % of the nephelometer data and 70 % of the aethalometer data were considered valid. All the AOPs had some gaps in the data (see Fig. 1). Most of these gaps in the time series of AOPs during the summers of 2009 and 2010 were due to too high RH. The gap in 2010 was due to maintenance and installation of the dryers and the switching inlet system. Some additional σ_{bsca} data were missing, due to malfunction of the backscatter shutter of the integrating nephelometer. Dirty optics, malfunctions and maintenance caused the gaps in the σ_{abs} data in 2012 and 2015.

Until March 2010, the integrating nephelometer and the aethalometer measured sample air that was not dried with any external dryers. During winter, the relative humidity (RH) remained below 40 %, since the sample air warmed up to room temperature (about 22 °C). Sometimes in summer, the RH of the sample increased to over the 40 % limit. If the RH was above 40 %, the data were flagged as invalid and they were omitted from the data analysis if not stated otherwise. About 25 % of all the data before March 2010 had to be removed due to too high RH. Almost all of the removed data was from summer and fall months (June – October) and if regarding only these months, 46 % of the data were flagged. If the moist data was included the overall data coverage would increase to 89 % and 77 % for scattering and absorption data, respectively. Monthly data coverage is presented in Table S1. After the installation of the Nafion-dryers in March 2010, the humidity caused no further problems."

P11L3: This is the first and last time ω_0 was discussed in Section 3.3. I am wondering if the four panels in Figure 4 showing ω_0 are needed at all.

We added discussion concerning the ω_o panel:

"Kulmala et al. (2016) estimated that fresh eBC particles observed at SMEAR II are in the size range of 80 – 120 nm. That estimate was calculated in a simplified way from the relationship between particle number

concentrations and BCe concentrations. A better estimate is obtained from the size dependence of ω_o. The darkest aerosol has ω_o < 0.6 and GMD in the range of about 30 – 70 nm (Fig. 3b, 3f, and 3j). This has been shown to be the range of fresh BC (e.g., Kittelson, 1998; Casati et al., 2007; Zhang et al., 2008) which suggests the source of BC is not far, probably within some kilometers only."

P11L21-24: The inverse proportionality between α_{sca} and GMD is supposedly caused by the bimodal size distribution of the aerosol and the substantial presence of accumulation particles. Despite supported by a reference, there is no direct explanation of the physical causes behind such proportionality. Since this is contrary to expectations, as stated by the authors, a deeper reasoning and explanation should be provided.

This was more and a detailed explanation is given in the Sect. S6 in the supplementary material. This was also described in the main text:

"To study the reasons behind this relationship we generated first unimodal size distributions with two geometric standard deviations GSD = 1.5 and 2.0 and calculated both σ_{sca} and σ_{bsca} at λ = 450, 550, and 700 nm with the Mie code with m = 1.517 + 0.19i and the α_{sca} and b from them. For unimodal size distributions the α_{sca} decrease with increasing GMD as is shown by the lines in Fig. 3c. Schuster et al. (2006) showed that the relationship may be the opposite for bimodal size distributions. Schuster et al. (2006) explained this behavior by that adding a larger or coarse particle size mode to a fine particle mode that is inefficiently scattering - for instance nucleation and Aitken mode particles – the larger mode contributes more efficiently to the Ångström exponent than the fine mode. The contribution of the particles smaller than 100 nm to GMD is larger than that of the larger particle modes which leads to the observed relationship. To study this in more detail we generated also bimodal size distributions. The analysis presented in the supplement (S4) shows that the α_{sca} of bimodal size distributions can be calculated as a linear combination of the α_{sca} of the modes, weighted by the fractions of σ_{sca} of the respective modes. This explains the increase of α_{sca} with growing GMD."

P12L7-10: The diameter of the particles is the driver for both α_{sca} and *b*, I have some difficulties in understanding the relevance of the findings described here.

The point here was to show that the *b* and α_{sca} are sensitive to different size ranges and that the bimodal size distribution for PM10 particles can make the examination of *b* and α_{sca} a bit complicated. For PM1 particles the variation of *b* and α_{sca} is easier to understand since the size distribution is closer to a unimodal size distribution:

"There was a negative correlation between the GMD and PM10 b (Fig. 3d) as expected, but the correlation was rather weak. On the contrary, the correlation between the VMD_{tot} and PM10 b was slightly positive (Fig. 3h). The negative correlation of α_{sca} with VMD_{tot} and the positive correlation of b with VMD_{tot} for the PM10 particles indicates that the α_{sca} and b were sensitive to different size ranges. The α_{sca} decreased when there are more coarse particles present, but for the b the coarse particles seem to have no expected effect and the b increased with increasing VMD_{tot}. Fig. 4a. shows that when the VMD > 1500 nm, the peak of $DV/dlogD_p$ in the accumulation mode was much lower and tilted towards the smaller diameters than compared to the situations where the VMD < 1000 nm. This is in line with Collaud Coen et al. (2007), who stated that in the Jungfraujoch data, b was sensitive to particles smaller than 400 nm and that the sensitivity of the α_{sca} was at its maxima for particle diameters between 500 and 800 nm.

For the PM1 particles, the measured α_{sca} and b were well in line with the modeled values (Figs. 3k and l), since the coarse mode particles were removed prior to the measurements, the shape of the size distribution was closer to a unimodal size distribution, and the VMD_{fine} described better how the accumulation mode shifted."

P13L2-3: Here is stated that long-range transport brings pollution to the station, but 70% of black carbon comes from local and regional sources (P13L7). These two statements are contradictory.

Here, I meant to say that the local and regional BC emissions are also important in winter. I formulated this paragraph to:

"Hyvärinen et al. (2011) observed increased equivalent black carbon (eBC, the BC concentration determined optically from σ_{abs} measurements) concentrations at SMEAR II in winter, when the long-range transport brings pollution from the central and eastern Europe. However, Hienola et al. (2013) estimated that about 70 % of the measured eBC at SMEAR II is emitted from local or regional sources or transported from Finnish cities so also the local and regional emissions have a significant role in the elevated eBC concentrations."

P13L4-5: I am not sure to understand the relevance of the polar dome here.

I formulated this sentence and removed the reference to polar dome. I meant that the southern air masses are more common at SMEAR II in winter, which brings pollution from central or eastern Europe.

P13L30-33: You have the size distribution data, why should you make a hypothesis on size distribution from optical properties?

I added a figure about the seasonality of the size distribution in the supplementary material so no hypothesis needs to be done.

*"The seasonal variation in α_{sca} and b depends on the seasonal variation in the size distribution of the particles. Both α_{sca} and b were maximal in summer and minimal in winter, suggesting that in summer, the particle population consisted of smaller particles than in winter. Closer investigation on the size distribution, which is presented in Fig. S3 and S4, reveals that in winter, the VMD_{tot} was experiencing it minimum due to a lack of coarse mode particles. This is in contrast with the observation or smaller α_{sca} and b. In fact, the seasonal variation of α_{sca} and b was explained by the seasonal variation of accumulation mod*e and VMD_{fine}, which is a good indicator for the shifting accumulation mode. *In winter, the accumulation mode was shifted towards larger sizes and the median of VMD_{fine} was about 350 nm. In summer the situation was the opposite and VMD_{fine} was about 250 nm."*

P15L15-18: Here you need to be careful with the instrumental error. Do you mean that absorption was close to the detection limit of the instrument or that dominant presence of non-absorbing particles caused a decrease of light transmitted through the filter and apparent absorption (Müller et al., 2011)?

I formulated this part. I meant the apparent absorption caused by scattering and how it causes relative large uncertainty since the scattering is high and absorption is low.

"The deviation of the σ_{abs} PM1/PM10 ratio clearly varied seasonally. In summer, the variation was considerably higher than in winter. In the correction algorithm, which was used for the absorption data (Eq. 3), part of the σ_{sca} is subtracted from σ_{abs} as an apparent absorption (Muller et al., 2011). This subtraction causes relatively high uncertainty when the σ_{abs} is low and σ_{sca} is high like it is in summer. This uncertainty is emphasized for PM10 measurements, since the σ_{sca} is relatively higher than σ_{abs} if compared to PM1 measurements. The uncertainty in the measurements also explains why there were so many values above 1 measured in the PM1/PM10 σ_{abs} ratio."

P15L23-24: The RFE trends are not described, discussed or interpreted. This recalls my major comments. The manuscript is loaded with data that are never discussed. Provide an interpretation or remove

I added more discussion in Sect. 3.6 about the trends and seasonal variation of RFE.

Fig.10a. By the way, add to all figures the panel reference.

Fixed this.

P15L26-28: Since RFE is calculated from b and ω_0 and all the environmental variables are kept constant, RFE must change with b and ω_0. As follow up to the second major comment, the authors are required to provide a deeper interpretation of their results.

We added more discussion about the effect of environmental variables and about the effect of the RH. See my answer 1.3 at the beginning of the document. Taking the seasonality of the environmental parameters into account amplifies the seasonal variation of RFE. The effect of RH is not as pronounced as the effect of using the seasonally varying environmental parameters.

P15L29: How the monthly RFE should be interpreted if the atmospheric and environmental parameters are kept constant? Moreover, it appears that the constants are not representative of SMEAR II. So, what should we really learn out of RFE?

More discussion about this in Sect. 3.6. As stated by Sherman et al. (2015), the RFE provides a means for comparing the intrinsic forcing efficiency of aerosols measured at different sites, this is the reason for calculating it by using the same constants that have been used in other publications.

P16L5-8: The problem here is that the aerosol optical depth is affected by RH and subsequent hygroscopic growth. So, all your RFE are systematically underestimated by an unknown factor. However, it is unclear if optical depth is measured or calculated.

Our study used only in-situ measurements of AOPs and we have not measured the AOD. I have emphasized this in the text:

"The RFE (or $\Delta F\delta^{-1}$) describes only the efficiency of the aerosol particles in cooling or warming the climate per unit of aerosol optical depth (δ). Eq. 11 assumes that the properties of the aerosol particles are uniform in the atmospheric column that is rarely the case in reality. In ambient air, we should also take into account the variability in RH as a function of height. At the top of the boundary layer we typically have RH values close to 100 %. Here, we determined the RFE by using the RH measured near the ground (16 m). The simplified RFE does not give an absolute value for the aerosol forcing, however, it can still indicate how the changes in AOPs affect the climate."

P16L9-10: Nessler et al. (2005) suggested that water uptake does not enhance absorption coefficient of BC.

I added a citation to this study and took this finding into account when determining the effect of ambient RH on the ω_o and further on to RFE.

P16L11-13: From this work, it is impossible to quantify the change of radiative forcing, nor the effects on the climate. First, RFE trends are not discussed: Second, the absolute values of RFE, as admitted by the authors, are far from being realistic. Moreover, why should we use RFE as "an indicator of how the properties of the aerosol particles have been changing" if the changes of aerosol particles have been measured (Section 3.2, 3.3, 3.4)?

I added here the RFE calculated by using more realistic values (see my answer 1.3). I also improved the discussion. The point of determining the RFE is not to quantify the radiative forcing (for that we would need a lot more parameters, AOD for example). However it describes how the efficiency of aerosol particles to cool (or warm) the climate has changed during the measurement period.

P17L1-2: Fig 1 and Fig. 2 show a net decrease of aerosol number concentration, but is this due to the implementation of new emission policies only? How did precipitation and air circulation changes from 2006? I would recommend the authors to consider all possibilities and base their final conclusions on their data and existing literature.

I formulated this:

"The extensive AOPs, as well as the aerosol number and volume concentration, tended to decrease. Our observation was in line with the other studies conducted in Europe and North America that also observed decreasing trends for the extensive AOPs (Collaud Coen et al., 2013; Pandolfi et al., 2018; Sherman et al., 2015), number concentration (Asmi et al., 2013) and aerosol optical depth (Li et al., 2014). This uniform decreasing trend in the amount of aerosol particles suggests that the anthropogenic emissions of particulate matter and gases that take part in secondary aerosol formation has been decreasing in Europe and North America The observed tendency for b and α_{sca} to increase indicated that the particle size distribution was moving towards smaller diameters. A more detailed investigation revealed that the number of larger accumulation mode particles decreased relatively the fastest, which also supports the assumed decrease in pollution."

F1: This figure is too crowded, I do not think that showing both PM1 and PM10 as any relevance (see major comments).

I removed the PM1 column from here.

F2: Here 5 panels are used to show that the total number of particles decreases and the size distribution is shifted to the smaller diameters. I would say that two panels will do efficiently the job. For example, one panel showing the total particle number concentration (Nfine+Ncoarse) and a second panel showing the ratio between Nfine and Ncoarse or the GMD. Note that Nfine is never defined in the text, is this accumulation+ Aitken+nucleation? Please provide a description.

I removed two of the panels. Now there are panels for total particle number concentration (N_{tot}), total particle volume (V_{tot}) and VMD_{tot}. We kept these parameters since *N* describes well the overall decrease in aerosol particles and *V* describes the amount of optically active aerosol matter. VMD was used instead of GMD, since it is more sensitive to changes in the optically active size ranges.

F1-2 As a follow up of my previous comments, I would find a way to merge together a reduced version of Figure 1 and 2, with the goal to focus on the relationship between physical and optical properties described in the text.

I see this point, but I could not merge these figures due to technical reasons (the figure became too crowded and the fonts too small). I would also like to keep the optical parameters separated from the size distribution parameters.

F3 This Figure is mentioned only once at P9L26, it does not appear to provide a key insight into the understanding of data interpretation. I would thus recommend to move it to the supplementary.

We removed this figure from the main manuscript according to your recommendation. However, we kept it in the supplementary material since it proves that the relatively highest decrease occurred in the larger side of the accumulation mode and thus supports the observed trends in increasing *b* and α_{sca}.

F5: The size distribution of PM10 contains all the necessary data to investigate the size distribution in PM1. This is clear in panels (c) and (d), where the size distributions below 1 um are exactly the same. This recalls my general comments, is a separated discussion of PM1 and PM10 really necessary?

In Figs. 4a and b we used different VMD values as limit values for averaging the size distributions. These values differ for PM1 and PM10 as well as do the *b* and α_{sca}. So if we want to study how the *b* and α_{sca} are related to the VMD, we need to investigate these separately for PM1 and PM10. However, since GMD is practically the same for PM1 and PM10, we now show the average size distribution limited by the GMD for the PM10 only. We also removed the panel where the PM1 AOPs were compared against GMD in the old Fig. 4.

F6: The figure shows the nucleation events and the related change in the real part of the refractive index. However, I think that it is largely overcrowded. On page 12, lines 26-27 sufficiently describe the absence of change in the observed AOPs. Due to the low relevance of AOPs variability in this context, I would suggest removing the third and fourth panels from the top. Finally, I am wondering what is the relevance of 2 months data over a 10 year period.

We removed this figure and the section discussing about it from the manuscript, since we realized that it is too much for this article.

REFEREE 2

GENERAL COMMENTS

This manuscript reports on the optical and microphysical properties of aerosols collected for over a decade at the SMEAR-II atmospheric monitoring station in Finland. These data are valuable in determining long-term trends and variabilities in aerosol properties, which are useful to climate modelers. The statistical distributions of aerosol properties presented in this paper should also be useful to GCM and CTM modelers for model initialization and validation exercises. As such, I think this paper is appropriate for inclusion in ACP and warrants publication after attention to the comments listed below.

The paper is well organized and there are only a few places were the English usage could be improved. The methodology used by the authors is excellent and of high quality, and the data presented are in general valid and relevant. I do have some comments that suggest some additional thought be given to provide better explanations of the observations, and I think a better discussion of how drying the sampled aerosols might influence the RFE results is warranted (see comments below).

The paper is a bit long but the amount of data being presented from over a decade at this site and the necessary discussions warrant a longer paper. In looking for possible ways to decrease the length of the paper, the only thing I see is to remove the size distribution discussion. While it is interesting in its own right and assists in the interpretation of the AOP data, it is not strictly necessary in this paper. I will leave that decision up to the authors and the editor.

We have now kept the size distribution section since they explain the behavior of AOPs. However, we cut some other elements (Sect. 3.3.1 and 3.5) from the manuscript to shorten it a bit and to emphasize important results.

In order to better interpret trends and variability, some estimates of the measurement uncertainty should be provided. I would point the authors to the work of Sherman et al. (2015, ACP), who put a great deal of effort into estimating measurement uncertainties for aerosol optical properties. There is no need to repeat this exercise in detail, but at the very least this reference should be included and some mention of the measurement uncertainties for the TSI nephelometer should be provided.

We cited this work concerning the uncertainty of the Nephelometer. Since they used PSAP in measuring absorption, we determined the uncertainty of the Aethalometer in a similar manner to Backman et al. 2017. We determined that the uncertainty of the σ_{abs} was about 23 %.

It was a bit disappointing to find little or no discussion in sections 3.1-3.3 on the relevance and importance of the measurements and their long-term trends and variability. A considerable amount of discussion is presented in sections 3.4-3.7 to explain the seasonal and diurnal variability, etc., and I would like to see more of this in sections 3.2 and 3.3. For the trends, for example, it would be useful to know how these trends compared with other long-term trends in Europe. The Pandolfi paper is cited and is an excellent place to start. Some additional information can be found in Collaud-Coen et al. (2013, ACP), and this paper should also be cited when comparing the optical property (scattering and absorption) measurements.

We have now added discussion to these sections, especially to Sect. 3.2.

There is also little discussion on the importance of measuring the optical properties in two different size ranges (PM1 and PM10). What does it tell you about sources, ageing, human contribution, etc., if the PM1 fraction for a given parameter is almost as large as the PM10 fraction? What does it mean if the PM1/PM10 ratio is changing over time? The authors went to the trouble of adding this additional set of PM1 measurements in 2010 and have several tables and graphs in this paper showing the results. They need to say why they are important and what we learn from them.

We added a motivation to measure PM1 to the introduction:

"The measurements of AOPs were started for aerosol particles smaller than 10 µm in diameter (PM10). The PM10 measurements are sensitive to coarse particles that are typically primary and originated from natural sources, such as soil dust and sea salt. To obtain additional information about submicron particles, parallel measurements of AOPs for PM1 were launched in June 2010. Motivation to measure also PM1 particles is that secondary aerosols (both natural and anthropogenic), and anthropogenic primary aerosols are typically submicron particles. Having measurements for different cut-offs makes the measurements also more comparable between different stations, since stations might use different cut-off sizes."

The purpose of the lengthy discussion of the comparison of the optical and microphysical properties on page 11 is not clear to me. The manuscript title indicates that this manuscript is about the aerosol optical properties, so why are there size distribution data included in the results and discussions? They are of course useful for interpreting the optical properties, so they have value, and good agreement between measured optical properties and ones calculated from the microphysical measurements give increased confidence in the findings of the study. Perhaps the authors can state that more clearly. The size distribution results could also go in the supplemental materials section if length of the paper becomes a concern.

We have kept the size distribution study in the manuscript since the size distributions explain most of the optical properties. The size distribution measurements are independent from the optical measurements so together they increase confidence to the results. We even added some discussion of the size dependence of single-scattering albedo as wished by the other reviewer. Another addition is an explanation of the increasing Ångström exponent with increasing geometric mean diameter as also wished by the other reviewer. That analysis is in the supplement.

The RFE calculations in this paper use the global average constants of Haywood and Shine rather than ones estimated or derived for the local area. This is probably OK for trend analysis but the magnitude of the forcing is wrong, especially when considering seasonal variations. For example, the constant used for the global average surface albedo (0.15) does not represent that of the boreal forest around SMEAR-II station over all seasons… it should be significantly higher in winter due to snow cover and (I would guess) lower in summer.

As stated by Sherman et al. (2015), the purpose of determining the RFE is to provide a means for comparing the intrinsic aerosol forcing efficiency of aerosols measured at different sites. We calculated the RFE by using the constant values to have results comparable with other studies in very different types of environments (e.g. Sheridan and Ogren, 1999; Andrews et al., 2011; Sherman et al., 2015; Shen et al., 2018) and to study how the RFE changes with varying ω_0 and b. However, we have now determined RFE also by using more realistic environmental parameters also. See my answer 1.3 at the beginning of this document.

Also, the measurement relative humidity (RH) and the ambient RH were generally different (this occurred most frequently in the summers). The authors state that if the sample RH was above 40%, the data were flagged and marked as invalid. This implies that the SSA and b values are only accurate when the ambient RH was low (i.e., close to the measurement RH), and that the RFE results are only appropriate for times when the ambient RH was low. Aerosol hygroscopic growth is generally thought to increase the ambient light scattering coefficient much more so than the ambient light absorption coefficient, which would lead to a higher single scattering albedo and, most likely, a more negative top-of-the-atmosphere RFE value (i.e., stronger cooling effect). If the ambient RH was higher in many cases than the measurement RH and these measurements were removed from the data set, the reported data set is biased toward a smaller (less negative forcing) cooling effect. Given that the RFE values are most likely not representative of the SMEAR-II region (they use the global average constants) or actual atmospheric conditions, I question their value in this manuscript. If they are to be kept, the authors should re-emphasize that the RFE results are technically meaningful only in the trend analysis (in Table 3) and that the calculations are for dried aerosols using global average constants and thus considerable caution should be used when trying to interpret seasonal variation in RFE at SMEAR-II (Fig. 10). The RFE results could also be moved into the supplemental materials if length of manuscript is a concern.

We have now estimated the ω_o and b for ambient RH as well and taken this into account in the RFE calculations. See my answer 1.3 at the beginning of this document for a more detailed description.

SPECIFIC COMMENTS

Pg. 1, Line 14: Replace the words 'affected to' with 'influenced'.

Fixed.

Pg.1, Lines 20-21: 'For the aerosol particles to have a cooling (warming) effect, the reflectivity of the particles must be higher (lower) than the albedo of the surface…'. What is the definition of 'reflectivity' the authors are using (or is it being used in a qualitative sense here)? For aerosol particles, are the authors referring to

aerosol single-scattering albedo (SSA) or some other reflective properties of the particles? It is not technically correct to state that '…the aerosol particles… have a cooling (warming) effect (if) the SSA of the particles (is) higher (lower) than the albedo of the surface…'. Solar photons can be elastically scattered in the forward direction, which does not appreciably cool the surface or lower atmosphere. I would recommend removing this sentence as it is not really necessary anyway, but if kept in the manuscript the authors should state how they are defining the term 'reflectivity' and how that is being compared to surface albedo.

I reformulated this part.

Pg. 2, Line 6: Replace 'concentration' with 'mass and/or volume'. Extensive AOPs are not dependent on the concentration of the particles but on the amount of aerosol present. Freshly formed particles may have extremely high concentrations in the atmosphere and show very low scattering values.

Replaced.

Pg. 2, Line 8: Replace 'concentration' with 'amount of aerosol'. Same explanation as above.

Replaced this as well.

Pg. 2, Line 11: Eliminate '…and not only on the amount of scattering and absorption.'

Eliminated.

Pg. 2, Lines 27-28: Why is it important to measure the AOP's of PM1 particles? This should be stated in the manuscript somewhere.

We added a motivation to measure PM1 particles in the introduction (see my answer to one of the major comments).

Pg. 3, Line 13 and Line 23: When will the Luoma et al. manuscript in preparation be available? Will it be available by the time this manuscript is published? If not, other references on how the various instruments compare would be appropriate.

I had too optimistic expectations about the timetable with that manuscript… I have removed self-citation from the manuscript and modified the text.

Pg. 3, Lines 19-22: The reported AOP's will vary depending on the measurement conditions. The direct aerosol radiative forcing effects at SMEAR-II, however, depend on the ambient conditions of T, P and RH, which were not usually the same as the measurement conditions. A discussion of how this would affect the results is appropriate. Are your seasonal results biased by a) eliminating the high ambient RH periods (which occur more frequently in the summer) before the driers were installed in 2013, or b) accepting these periods after 2013

with high ambient RH but reduced measurement RH? Some discussion of the fraction of data flagged as invalid due to high ambient RH before 2013 is warranted, as is the fraction deemed acceptable (with significant drying) after the driers were installed. This way the reader can understand if this was a frequent or merely occasional occurrence.

The RFE does not depend on T or p, since it is an intensive property. But it does depend on the RH and I have now taken this into account in the paper. I added median values of other AOPs including the high RH conditions as well. I also added a more detailed description about the fraction of invalidated data in the new "2.3.4 Data coverage" section.

I now did the trend analysis for a data set, where the high humidity conditions were included. The trends did not change remarkably compared to the data set, where the moist conditions were excluded. I had a typo in the old manuscript concerning the installation of the driers. The driers were installed already in 2010, not in 2013, so there were only four years of measurements without the drier.

Pg. 4, Line 2: How warm does the sample air to the APS instrument get? Does this heating to above room temperature remove any volatile species other than water (e.g., ammonium nitrate)?

The sample air is heated to 40 °C and for example ammonium nitrate would be evaporated, however, the concentration of ammonium nitrate is very low in Hyytiälä so this should not affect in our study. Alternatively, there are many other volatile compounds at SMEAR II. These compounds take part in the secondary aerosol particle formation and the resulting particles are typically smaller than what we measure with the APS. Thus we believe that heating the sample up to 40 °C has no significant effect here.

Pg. 4, Lines 11-12: 'We did not apply the truncation correction to the backscattering, since the backscattering measurements were much noisier, especially at the red wavelength.' OK then the determination of *b* is wrong, as is the calculation of the upscatter fraction, and the question is how far off are your values from the fully truncation corrected values. An estimate of the uncertainty or error that enters the calculation of *b* due to not applying the truncation correction to the σ_{bsca} values should be given. I agree that the s σ_{bsca} values are quite noisy at 1-minute resolution. At what resolution were you recording the raw data (1 second?,1 minute?, 10 minutes?, I don't see this listed in the manuscript)? Could you have averaged the σ_{bsca} values to hourly or longer resolution before applying the corrections? This would perhaps help to beat down the noise a little.

Backscattering data has now been corrected as well.

Pg. 4, Lines 18-23: Which algorithm(s) or recommendations in Collaud Coen et al. (2010) were used? In that paper they evaluated four previous aethalometer correction schemes (Weingartner, Arnott, Schmid and Virkkula) and they also made new recommendations on the applicability of each in different circumstances.

We used the new recommendation presented in that paper. I added a better description about the correction algorithm we used.

Pg. 5, Line 12: Replace the word 'direction' with 'hemisphere'.

Replaced.

Pg. 5, All equations: The subscript font is quite small. Possibly it will look better in the published version.

I have now increased the font a bit for so that it is easier to review.

Pg. 4-6, Section on Data Processing: Somewhere in this manuscript the authors need to give some estimate of the measurement uncertainties of the instruments they are using. I recommend looking at the work of Sherman et al. (2015, ACP) to see how they calculated the measurement uncertainties. It is a lot of work so I do not recommend that you try to repeat those analyses, but you should be able to reference their Table S2 'Total and precision fractional uncertainties (%) of measured PM1 and PM10 aerosol optical properties (AOPs) σ_{sp}, σ_{bsp}, and σ_{ap} and calculated AOPs (e.g., the intensive AOPs) for 1-hour averaging time. Uncertainties are expressed as 95% confidence intervals.' and state the uncertainties relevant to your report.

We have now added the uncertainty of the Nephelometer in the manuscript and we estimated the uncertainty of the Aethalometer in Sect. 2.3.2. An estimation for the intensive AOPs is presented in the supplement.

Pg. 6, Line 8: '…the absorption would be dependent on wavelength as lambdaˆ-1…'. Rephrase as '…the absorption would have a wavelength dependence of approximately lambdaˆ-1…'.

Rephrased this.

Pg. 6, Lines 28-29: While adjusting the AOP's to a common set of conditions is appropriate (and indeed necessary) to evaluate trends and to compare properties at different sites, you need the measurements at ambient conditions to determine the effects of aerosols on perturbing the surface radiation balance (i.e., their direct radiative/climate forcing effect). It would be good to provide some estimate or limit as to how different the AOP's are for dried vs. ambient air. Perhaps an example calculation, where the AOP's are adjusted to ambient conditions using some assumed conditions of T, P and RH, would help. I am sure there are studies of Finnish/Scandinavian/northern European aerosols where the aerosol hygroscopic growth was measured or calculated. These results could be used as a very rough scaling factor to calculate the AOP's at SMEAR-II at ambient atmospheric conditions. Otherwise the reader will not know if the presented dry aerosol RFE results are even close to those for real atmospheric conditions at SMEAR-II.

We did more analysis on RFE, where we took the seasonality of the D, R_S, and A_C into account. We also determined the RFE for ambient conditions by calculating the b and ω_0 for moist conditions. See my answer 1.3 for a more detailed description.

Pg. 7, Line 15: Replace 'describes' with 'provides information on'.

Replaced.

Pg. 8, Line 3: Replace 'chapter' with 'section'.

Replaced.

Pg. 8, Line 15-16: 'Naturally, the different methods used in the absorption data processing also affected the optical properties, which are dependent on the sigma-abs, such as ω_0 and k.' How much of a difference in ω_0 or k can be attributed to the different data processing methods? Is it a large or small difference? Could you provide an example where the same processing is used in two different time periods that shows how large of an effect this is?

Table S2 in the supplementary material presents various absorption depended AOPs that were determined from absorption data that was corrected using the correction algorithm by Arnott et al. (2005). In this correction algorithm we used the same C_{ref} as Virkkula et al. (2011). Compared to Virkkula et al. (2011), we used a corrected spot size and flow, and we invalidated situations when the RH > 40 % (Virkkula et al. (2011) invalidated situation when the RH > 50 %). The RH limits for acceptable data were taken from WMO GAW recommendations. In the GAW guidelines of 2003 the recommendation was to maintain RH < 50% but the limit was later lowered to RH < 40% (WMO/GAW, 2003, 2016).

The absorption at 520 nm was similar for both corrections but at other wavelengths the were differences. At lower wavelengths the σ_{abs} was higher for the data that was corrected by the Arnott et al. (2005) algorithm. At higher wavelengths the situation was the opposite. Thus there was a notable change is in the α_{abs} that describes the wavelength dependency of σ_{abs} and the α_{abs} was 1.4 for the σ_{abs} data that was corrected by the Arnott et al. (2005) algorithm. For other σ_{abs} depended parameters there were no significant differences at green wavelength. We did not do the analysis for the *k* since running the iteration for the whole data set takes a long time and we expected to see no large differences.

Pg. 9, Line 6: Replace 'marked' with 'included'.

Replaced.

Pg. 9, Section 3.2, second paragraph: The 13%/year decrease in the σ_{abs} value at SMEAR-II is an important finding and should be emphasized here! Has this been observed at other sites in Finland and/or Europe? Can you provide a hypothesis as to why this happened over the last decade at SMEAR-II station? Could it be more local or regional/continental scale effects? Is it due to less soot aerosols? Or possibly decreasing amounts of BrC?

I do not think that there has been this steep decrease in other rural or remote stations or at least I could not find any citations. The trend of absorption in PM1 aerosol was calculated for only 7.5 years of data and it is more sensitive to extreme values in the time series. Here I believe the steep slope was caused by few extreme high values measured at the beginning of 2012. I find the trends calculated for the PM10 data more reliable since it is calculated for over a ten year period. I added some discussion about this difference in the results.

"For the PM1 σ_{abs}, we observed a very steep decrease (-12 %yr^{-1}), which was probably caused by very high σ_{abs} measured in January and February in 2012. Also the data gaps in winter 2013 and 2015 could have affected the

trends. The time series, of which the trends were determined for the PM1 measurements, were only 7.5 years long. Trends, which are determined for shorter time series are more sensitive to year-to-year variability. This kind of extreme values can induce relatively large trends, which is why trend analysis for short time series (less than ten years) should be treated with caution."

Pg. 13, Line 3: Replace 'means' with 'suggests'.

Replaced.

Pg. 14, Section 3.6, second paragraph: The difference in the PM1/PM10 scattering ratio between Virkkula (2011) at 85% and the current study at 75% is a little concerning. There could have been long term changes in the environment at SMEAR-II region that might partially explain this, or it could be a difference in sampling conditions. Was there any RH measurement made at or near the impactors (as opposed to inside the nephelometer)? You need an RH measurement taken near the impactors to ensure you have a proper size cut (i.e., without the possible artifact you mention).

Unfortunately we do not have any RH measurements near the impactor or the inlet. The impactor is inside the measurement cottage so the air has some time to warm up to room temperature (about 22°C). Of course it does not help during the summer, when the temperature outside is similar to the room temperature. The difference that we observe between these two studies could have been caused by some technical issues like this.

Another thing is that Virkkula et al. (2011) determined the ratio from scattering calculated with a Mie model from size distributions measured with the DMPS and the APS. In the present work it was determined from the scattering measured with the nephelometer with the alternating PM1-PM10 inlet. In the present work we omitted the PM1/PM10 ratio calculation from Mie modeling, however, so the ratios are not strictly comparable. Both approaches have fairly large uncertainties associated with the large particles.

Pg. 15, Section 3.7: It needs to be stressed that the RFE calculations are for dry or semi-dry (RH<40%) aerosols.

I have tried to stress this in text. But now there are also RFE calculated for more realistic conditions and ambient moisture.

Pg. 15, Line 23: '…, which makes the RFE decrease.' After decrease, add the parenthetical phrase '(i.e., become more negative)'.

Added the phrase.

Pg. 15, Line 26: Replace 'ine' with 'in'.

Replaced.

Pg. 16, Lines 5-13: This is a good explanation! The authors state that while the magnitude of the RFE perturbation cannot be precisely determined using this methodology, the trends probably can, and the RFE estimates they provide are most likely a lower limit to the true cooling effect.

Pg. 16., Lines 18-23, and Fig. 12: This is a discussion of systematic variability of aerosol optical properties. This type of systematic variability has been observed before. The earliest paper I know of that discussed this was Delene and Ogren (2002, J. Atmos. Sci, Fig. 8) which should be referenced. This was also in Sherman et al. (2015, ACP, Figs. 10a, 10b, 10d). Their results are consistent with those presented in this paper.

I added the citations here and included some discussion too.

"These relationships were also observed in a study of AOPs at the Station for Observing Regional Processes of the Earth System (SORPES), a measurement station in Nanjing China (Shen et al., 2018). Also, Delene and Ogren (2002) and Sherman et al. (2015) observed similar systematic variability between σ_{sca}, ω_0, b, and $RFE_{H\&S}$ at several North American measurement stations; when the σ_{sca} increases, the ω_0 increases and the b decreases. Sherman et al. (2015) suggested that this variability could be caused by deposition of larger particles, which typically absorb less light. Delene and Ogren (2002) observed that $RFE_{H\&S}$ increases (i.e. becomes less negative) with increasing σ_{sca}, but Sherman et al. (2015) did not observe this trend. "

Pg. 27, Fig. 3: The largest decrease over time is for the larger accumulation mode particles (i.e., 0.4-0.7 micrometer diam). Any ideas why?

I added some discussion here. The larger accumulation mode particles could be aged pollution particles that have been grown by SO_2 for example. The emissions of SO_2have decreased, which would support this claim.

"The results, which are presented in Fig. S3, pointed out that relatively greatest decrease occurred for accumulation mode particles that were 500 – 800 nm in diameter. On average, the volume size distribution of accumulation mode particles peaks around 300 nm (see Figs. S3 and S4) so the greatest decrease occurred at the larger sizes of the accumulation mode. The decrease in this size range might be caused by decrease in long-range transported pollution. Aged pollution particles might be grown by other substances, such as SO_2 in the atmosphere so their sizes are larger than freshly emitted or formed particles. SO_2 emissions have decreased in Europe (Tørseth et al., 2012), which supports this assumption. A trajectory analysis by Virkkula et al. (2011) showed that α_{sca} was clearly higher in air masses from continental Europe than from the North Atlantic and but also that the highest α_{sca} values were measured in air masses sources from within southern Finland, which would suggest that larger particles are not from nearby the station."

Pg. 29, Fig. 5: The text in the legends are very small. This may, however, be acceptable to the technical editor.

I have modified the figure and also made the legends bigger.

Pg. 31, Fig. 7: Why are there breaks in the whiskers and some whiskers not attached to the boxes? Is this a plotting artifact or is additional explanation necessary as to what the whiskers are meant to display?

I fixed this. The whiskers were drew with dashed lines, which caused them to be not attached to the boxes like you noticed in your next comment.

Pg. 33, Fig. 9: It appears that the whiskers are drawn as dashed lines with relatively long dashes and breaks. These should either be changed to solid lines or else changed to broken lines with smaller breaks in them.

Fixed this by drawing the whiskers with solid lines.

Pg. 35, Fig. 11: Caption '…1000 grid points in total.' Should this be '10,000 grid points in total.'?

Yes it should! I fixed the number.

Over a ten-year record of aerosol optical properties at SMEAR II

Krista Luoma[1], Aki Virkkula[1,2], Pasi Aalto[1], Tuukka Petäjä[1] and Markku Kulmala[1]

[1]Institute for Atmospheric and Earth System Research, University of Helsinki, Helsinki, 00014, Finland
[2]Finnish Meteorological Institute, Helsinki, 00560, Finland

Correspondence to: Krista Luoma (krista.q.luoma@helsinki.fi), Aki Virkkula (aki.virkkula@fmi.fi)

Abstract. The aerosol optical properties (AOPs) describe the ability of aerosols to scatter and absorb radiation at different wavelengths. Since the aerosol particles interact with the radiation from the sun, they also have an impact on the climate. Our study focuses on the long-term trends and seasonal variations of different AOPs measured at a rural background station in Northern Europe. To explain the observed variations in the AOPs, we also analyzed changes in the aerosol size distribution. AOPs of particles smaller than 10 µm (PM10) and 1 µm (PM1) have been measured at SMEAR II, in Southern Finland, since 2006 and 2010, respectively. For the PM10 particles the mean values of the scattering and absorption coefficients, single-scattering albedo, and backscatter fraction at λ = 550 nm were 15.2 Mm^{-1}, 2.1 Mm^{-1}, 0.87 and 0.14. The scattering and absorption Ångström exponents at the wavelength ranges 450–700 nm and 370–950 nm were 1.80 and 0.95, respectively. Statistically significant trends were found for example for the PM10 scattering and absorption coefficients, single-scattering albedo, and backscatter fraction, and the slopes of these trends were -0.32 Mm^{-1}, -0.086 Mm^{-1}, $2.2 \cdot 10^{-3}$, and $1.3 \cdot 10^{-3}$ per year. The tendency for the extensive AOPs to decrease correlated well with the decrease in aerosol number and volume concentration. The tendency for the single-scattering albedo and backscattering fraction to increase indicates that the aerosol size distribution consist of less larger particles and that aerosols absorb relatively less light than before. The trends of the single-scattering albedo and backscattering fraction influenced the effective aerosol forcing efficiency, indicating that the aerosol particles are scattering the radiation more effectively back into space.

1 Introduction

Aerosol particles directly affect the climate by scattering and absorbing the shortwave radiation from the sun (ARI, *aerosol–radiation interaction*) (Charlson et al., 1992). Aerosol particles can either have a warming or cooling effect on the climate, depending on the optical properties of the aerosol particles and the surface below the aerosol layer. ~~The ARI is dependent on the reflectivity of the aerosol particles as well as on the albedo of the surface below the aerosol layer. For the aerosol particles to have a cooling (warming) effect, the reflectivity of the particles must be higher (lower) than the albedo of the surface (Haywood and Shine, 1995).~~ Aerosol particles also affect the climate via aerosol–cloud interactions (ACIs) since aerosol particles may act as cloud condensation nuclei (CCN). By functioning as CCN, aerosol particles also affect the optical properties of the cloud (Haywood and Boucher, 2000). The more CCN are available, the smaller and more numerous are the cloud droplets. Clouds with more droplets scatter light more efficiently, so they have a larger cooling effect than clouds that

have fewer droplets (Twomey, 1991). Clouds with smaller droplets have longer lifetimes, since it requires more time for the cloud droplets to grow to the size of rain drops (Lohmann and Feichter, 1997). Longer lifetimes also increase the cooling effect of the clouds.

There are vast uncertainties in determining the global radiative forcing related to aerosol particles (Boucher et al., 2013). The number concentration, chemical composition and size distribution of aerosol particles vary widely both spatially and temporally, so it is challenging to consider them in the models. Challenges arise even more with the ACIs that include highly complex processes.

The aerosol optical properties (AOPs) describe how much the particles scatter and absorb radiation at different wavelengths. It is essential to know how the aerosol particles interact with radiation to determine the direct effect on the climate. The extensive optical properties, such as scattering and absorption coefficients, are dependent on the mass and/or volume of the particles and also on their size distribution and chemical composition. Intensive properties, however, are not dependent on the amount of aerosol but on the properties of the particles, such as the size distribution and composition. Intensive properties ~~can be determined by comparing~~are calculated from the scattering, backscattering and absorption measurements at different wavelengths. Therefore, by measuring the AOPs at different wavelengths, we can also obtain indirect information on the size distribution and chemical composition of the aerosol particles. ~~This explains why the measurements of AOPs can give practical results.~~

In situ measurements of AOPs have been conducted at SMEAR II (Station for Measuring Ecosystem–Atmosphere Relations; Hari and Kulmala, 2005) in Hyytiälä, Finland since 2006. SMEAR II is located in the middle of a pine forest and represents the atmospheric conditions typically found in boreal forests (Hari et al., 2013). Boreal forests are sources for new aerosol particles that are formed in a gas-to-particle conversions (Kulmala et al., 2004; Kulmala et al., 2013). Boreal forests (also known as Taiga) cover approximately 30 % of the world's forests and 8 % of the earth's surface, so they greatly affect the global radiation budget.

The measurements of AOPs were started for aerosol particles smaller than 10 µm in diameter (PM10). The PM10 measurements are sensitive to coarse particles that are typically primary and originated from natural sources, such as soil dust and sea salt. To obtain additional information about submicron particles, parallel measurements of AOPs for PM1 were launched in June 2010. Motivation to measure also PM1 particles is that secondary aerosols (both natural and anthropogenic), and anthropogenic primary aerosols are typically submicron particles. Having measurements for different cut-offs makes the measurements also more comparable between different stations, since stations might use different cut-off sizes. To study the causalities between the AOPs and the size distribution, we have also included the measurements of aerosol size distribution to our study.

Here, we present the observed temporal variation and trends of the AOPs at SMEAR II. These AOPs have been previously discussed by Virkkula et al. (2011) and Pandolfi et al. (2018). Virkkula et al. (2011) used the integrating nephelometer and the aethalometer data from a 3-year period (2006–2009). Pandolfi et al. (2018) compared the aerosol scattering measurements that were conducted at different measurement sites in Europe. At SMEAR II, the study involved nephelometer data, from 2006 to 2015. However, these articles determined the AOPs of the PM10 particles only, and Pandolfi et al. (2018) did not include absorption data. Long time series (2006–2017) of the measurements of both scattering and absorption together at SMEAR II have not been presented before, nor have the optical properties of the PM1 particles.

2 Measurements and methods

2.1 The field site

The measurements presented here were conducted at the SMEAR II station in Hyytiälä, southern Finland (61° 51' N, 24° 17' E, 181 m above sea level.). SMEAR II is located in the middle of a forest that consists mostly of Scots pine (*Pinus sylvestris* L.) trees (Hari et al., 2013). The nearest larger cities, Tampere (220 000 inhabitants) and Jyväskylä (140 000 inhabitants), are located about 60 km and 100 km from the measurement station. Otherwise, the area is sparsely populated and there are no large pollution sources nearby the station.

2.2 Instrumentation

2.2.1 Measurements of aerosol optical properties

AOPs have been measured at SMEAR II since June 2006. The measurements of aerosol scattering, backscattering and absorption coefficients (σ_{sca}, σ_{bsca} and σ_{abs}) were conducted at several wavelengths using an integrating nephelometer (TSI model 3563) and an aethalometer (Magee Scientific model AE-31), since 2013 also with a Multi-Angle Absorption Photometer (MAAP, Thermo Scientific model 5012). The nephelometer measures scattering at blue, green and red wavelengths (450, 550 and 700 nm) and the aethalometer measures absorption at seven wavelengths ranging from the ultraviolet to the near-infrared (370, 470, 520, 590, 660, 880 and 950 nm). Here, absorption data from the AE-31 and scattering data from the TSI3563 were used since they have the longest time series, and an important part of our discussion is the analysis of trends. We used the MAAP data in determining a multiple scattering correction factor for the Aethalometer to get more accurate absorption measurements.

Both scattering and absorption measurements were recorded with a 5 minute resolution before June 2010 and after that with a 10 minute resolution. From June 2006 to June 2010, the measurements were conducted for the PM10 particles only and since

June 2010 also for the PM1 particles. The sample air is taken through a PM10 inlet (Digitel, Low volume inlet) and led alternatingly either directly to the instruments or via an impactor that removes particles larger than 1 µm in diameter.

2.2.2 Size distribution measurements

In addition to the AOPs~~optical measurements~~, ~~measurements of the~~ particle size distribution data were used in the analyses below. The size distributions ~~measurements~~ were ~~conducted~~measured with a Twin Differential Mobility Particle Sizer (TDMPS) in the size range 3–1000 nm (Aalto et al., 2001) and a TSI Aerodynamic Particle Sizer (APS, Model 3321) in the size range 0.53–10 µm. In the overlapping range of the TDMPS and the APS the number concentrations from the TDMPS were used up to 700 nm. The TDMPS, APS, integrating nephelometer and the aethalometer are located in the same measurement building. The TDMPS and APS have their own individual measurement lines. In the TDMPS measurement line, there is an inlet that removes particles larger than 1 µm. There is no active drying system in the TDMPS sample line to prevent particle losses. However, the sheath flows, which are used in the TDMPS system, are dried (RH < 40 %) so the particles are sampled in dry conditions. In the APS measurement line there is a pre-impactor that removes particles larger than 10 µm. The APS has its own dryer that heats up the sample air to 40 °C. This temperature might evaporate some semivolatile compounds, for instance ammonium nitrate but this is mainly an issue of urban sites (e.g. Bergin et al. 1997), whereas at the forest site in Hyytiälä low-volatile organic compounds are common (Ehn et al., 2014). Nevertheless, semivolatile aerosol particles are typically secondary particles smaller than 1 µm in diameter so evaporation of them does not have a large effect on the APS measurements.

2.3 Data processing

The data used in this study were measured between 21 June 2006 and 31 December 2017. All the optical data were quality assured manually and averaged for 1 h periods. The aerosol hygroscopic growth is often significant when RH increases above ~45 ± 5% and therefore the World Meteorological Organization and Global Atmosphere Watch (WMO and GAW) recommend for aerosol monitoring stations to keep sample air RH lower than that. In the GAW guidelines of 2003 the recommendation was to maintain RH < 50% but the limit was later lowered to RH < 40% (WMO/GAW, 2003, 2016). In the present work, if the internal RH in any of the optical instruments exceeded 40 %, the data from that instrument were excluded from further analysis if not stated otherwise. Note that Virkkula et al. (2011) followed the earlier RH recommendation: they calculated AOPs using data measured at RH < 50%. In addition, they also presented results from data measured at all RH. This affects comparisons of the results presented in this work.

All the optical data were also converted from ambient conditions to the standard temperature and pressure (STP) conditions (1013 hPa, 0 °C).

2.3.1 Scattering data

Both total~~The~~ scattering and backscattering coefficients measured with the nephelometer ~~w~~were~~as~~ corrected for the truncation error according to Anderson and Ogren (1998). The truncation correction uses the Ångström exponent (see Sect. 2.3.3) calculated from the uncorrected data.

Sherman et al. (2015) presented a well documented analysis for determining the uncertainty of the different AOPs. They determined a total fractional uncertainty of 9.2 % and 8.9 % (8.0 % and 8.1 %) for PM10 (PM1) σ_{sca} and σ_{bsca}.

To test, if excluding the moist data had a large effect on the AOPs and their trends, we included the periods of high humidity (RH > 40 %) in some of the analyses. However, in these cases we corrected the scattering data, which was flagged due to too high RH, to dry conditions by using the scattering enhancement factor *f*(RH). *f*(RH) describes the increase of σ_{sca} with increasing RH

$$f(\mathrm{RH}) = \frac{\sigma_{\mathrm{sca}}(\mathrm{RH})}{\sigma_{\mathrm{sca}}(\mathrm{RH{=}\ dry})}. \quad (1)$$

f(RH) is the ratio of σ_{sca} measured at high RH and at dry conditions. The *f*(RH) can be described by empirical relationship

$$f(\mathrm{RH}) = q\left(1 - \frac{\mathrm{RH}}{100\ \%}\right)^{-\gamma}, \quad (2)$$

with a parametrization presented by Zieger et al. (2015) for aerosol particles measured at SMEAR II in summer. They determined mean values for q and γ that were 0.96 ± 0.07 and 0.24 ± 0.07 at red wavelength (450 nm), 1.01 ± 0.05 and 0.25 ± 0.07 at green wavelength (525 nm), and 1.01 ± 0.05 and 0.30 ± 0.08 at red wavelength (635 nm). We used this parametrization, when the RH was higher than 40 %. Zieger et al. (2015) presented parameterization for total scattering only so we did not correct the σ_{bsca} to dry condition.

This parametrization was also used for calculating the radiative forcing efficiency (see Sect. 2.3.3) in ambient RH.

2.3.2 Absorption data

The ~~aethalometer~~ reported flow by the aethalometer was corrected by comparing the flow ~~reported by the aethalometer~~ with the weekly flow measurements conducted at the station. The correction was applied by using a moving average of these

measurements (see Sect. S2.1). An average spot size diameter of 8.3 ± 0.~~1~~2 mm was measured from the old aethalometer filters by using a loupe measuring scale magnifier (Esch~~t~~enbach) with 0.1 mm accuracy and it was used instead of the spot size reported by the aethalometer.

Here, we corrected the Aethalometer data by using the correction algorithm described by Collaud Coen et al. (2010)

$$\sigma_{\mathrm{abs},i} = \frac{\sigma_{\mathrm{ATN},i} - a_{s,i}\bar{\sigma}_{\mathrm{sca},s,i}}{C_{\mathrm{ref}}\, L_{s,i}}, \quad (3)$$

where

$$L_{s,i} = \left(\frac{1}{l\left(1-\bar{\omega}_{0,s,i}\right)+1} - 1\right) \cdot \frac{\mathrm{ATN}_i}{50\ \%} + 1, \quad (4)$$

and

$$a_{s,i} = \bar{\zeta}^{d-1}_{\mathrm{sca},s,i} \cdot c \cdot \lambda^{-\bar{\alpha}_{sca,s,i}\cdot(d-1)}. \quad (5)$$

In Eqs. 3 and 4, the subscript *i* indicates the number of the measurement and the subscript *s* indicates the average properties of the aerosol particles that are embedded in the filter spot. The over lined parameters are mean values from the start of the filter spot to the *i*th measurement. In Eq. 3, the σ_{ATN} is the attenuation coefficient reported by the Aethalometer, a is the scattering correction parameter, C_{ref} is the multiple scattering correction factor, and L is the loading correction function. In Eq. 4, the ω_0 is the single scattering albedo (see Sect. 2.3.3) and the ATN is the light attenuation through the filter spot in percentages. In Eq. 5 the ζ_{sca} is the proportionality constant of the wavelength power law dependence of σ_{sca} and α_{sca} is the Ångström exponent of the σ_{sca} (see Sect. 2.3.3). For l, d, and c we used values 0.74, 0.564 and $0.329 \cdot 10^{-3}$ respectively. For scattering correction, we used measured σ_{sca} values that were interpolated and extrapolated to the AE-31 wavelengths. Note that most of the symbols used for the variables are different from Collaud Coen et al. (2010). The reason is that in the present work the symbols are used for other variables below.

The C_{ref} was determined by comparing the Aethalometer data, that was corrected only for the filter loading artefact, against the reference absorption coefficient ($\sigma_{\mathrm{abs,ref}}$) measured by the MAAP.

$$C_{\mathrm{ref}} = \frac{\sigma_{\mathrm{ATN}}}{L \cdot \sigma_{\mathrm{abs,ref}}}. \quad (6)$$

The resulted median value for C_{ref} was 3.19, with a standard deviation of 0.67.

The uncertainty of the σ_{ATN} was determined according to Backman et al. (2017)

$$\frac{\delta\sigma_{\mathrm{ATN}}}{\sigma_{\mathrm{ATN}}} = \sqrt{f_{\mathrm{A}}^2 + f_{\mathrm{Q}}^2 + \left(\frac{\delta\sigma_{\mathrm{ATN,zero}}\Delta t_{\mathrm{zero}}}{\sigma_{\mathrm{ATN}}\Delta t_{\mathrm{avg}}}\right)^2}, \quad (7)$$

where the f_A and f_Q are the fractional uncertainties of the Aethalometer spot size and flow, which we determined to be 4.9 % and 1.5 % respectively; $\delta\sigma_{ATN,zero}$ is the standard deviation of the zero measurements; Δt_{zero} is the averaging time of the zero measurements; and Δt_{avg} is the averaging time of the measuremetns. For the uncertainty of σ_{abs} we took into account the fractional uncertainty of the C_{ref} that was f_C = 21 %

$$\frac{\delta\sigma_{abs}}{\sigma_{abs}} = \sqrt{\left(\frac{\delta\sigma_{ATN}}{\sigma_{ATN}}\right)^2 + f_C^2}. \quad (8)$$

At 520 nm, the uncertainty of σ_{abs} ranges from 22 % to 24 % if the σ_{ATN} varies from 14.2 Mm^{-1} to 1.3 Mm^{-1}, which are the 10th and 90th percentiles of σ_{ATN}. In this estimation of uncertainty, we did not take the uncertainty of scattering correction into account.

In calculating the single-scattering albedo and in iterating the complex refractive index, the absorption data had to be interpolated to the same wavelength with the scattering measurements. The absorption data were then interpolated to the blue, green, and red -wavelengths (450, 550, and 700 nm), using the Ångström exponent (α) described in Eqs. 11 and 12.

2.3.3 Intensive optical properties

The extensive ~~properties~~AOPs, which are the scattering, backscattering, and absorption coefficients (σ_{sca}, σ_{bsa}, and σ_{abs}), were used to calculate intensive properties presented in detail below.

The single-scattering albedo (ω_0) describes how much of the total light extinction (sum of σ_{sca} and σ_{abs}) caused by the aerosol particles is due to scattering:

$$\omega_0 = \frac{\sigma_{sca}}{\sigma_{sca} + \sigma_{abs}} \quad (9)$$

The ω_0 can be linked with the source and chemical composition of the aerosol particles. High values of ω_0 mean that the aerosol particles are mostly scattering and are light in color. Darker aerosol particles, which have a lower ω_0, have a relatively higher mass fraction of absorbing material, such as soot that is emitted in combustion processes.

The backscatter fraction (b) describes how much aerosol particles scatter radiation in the backward hemisphere compared with the total scattering

$$b = \frac{\sigma_{bsca}}{\sigma_{sca}}. \quad (10)$$

The angular dependency of particle scattering is dependent mostly on the particle size. The value of b is smaller for a size distribution that consists of larger particles, since large particles scatter light heavily in the forward direction and thus b can be used as an indicator of the shape of the particle size distribution. The b is an especially important property for modeling the

direct effect of aerosol particles on the climate, since it is used to describe how much sunlight is scattered upwards back into space.

The Ångström exponent (α) is used to describe the wavelength (λ) dependency of a certain optical property (σ) (Ångström, 1929)

$$\alpha = -\frac{\ln\frac{\sigma_1}{\sigma_2}}{\ln\frac{\lambda_1}{\lambda_2}}. \quad (11)$$

After calculating α, the optical property can be extrapolated or interpolated into different wavelengths

$$\sigma_1 = \sigma_2 \left(\frac{\lambda_1}{\lambda_2}\right)^{-\alpha}. \quad (12)$$

In this study, α values were calculated for σ_{sca} and σ_{abs} to obtain α_{sca} and α_{abs}.

Since light scattering is highly dependent on particle size, α_{sca} is also used as an indicator of the particle size distribution and is larger for the smaller particles, since they have a stronger wavelength dependency. If α_{sca} is larger than 2, ~~it is typically believed that~~ the volume distribution is typically dominated by particles smaller than 0.5 µm, and if α_{sca} is smaller than 1, ~~the~~ larger particles (physical diameter D_p > 0.5 µm) predominate in the distribution (Schuster et al., 2006). In comparison to b, α_{sca} is more sensitive to the coarse mode particles (e.g. Collaud Coen et al., 2007).

The value of ~~α_{abs} is also dependent~~depends also on the chemical composition, coating, and size of the particles, even though the chemical composition is generally considered to be the more important factor. The α_{abs} is usually used to identify black carbon (BC) and brown carbon (BrC) particles. The BC particles are highly absorbing aerosol particles and the BrC particles are considered to consist of some organic carbon compounds that absorb light more strongly at short than long wavelengths. If the particles consist purely of BC, the absorption would have a wavelength dependence of approximately λ^{-1} and α_{abs} would be equal to unity. However, if the particles also consist of material that absorbs light only at ultraviolet wavelengths, α_{abs} would be larger than 1. In ageing processes the BC particles may become coated by some purely scattering material, such as sulfuric acid or ammonium sulfate, or by slightly absorbing organic material (Schnaiter et al., 2005; Zhang et al., 2008). The coating greatly affects the absorption wavelength dependency, and thus the division into BC and BrC by considering only α_{abs} is not that simple. If the sizes of the BC particles and the thickness and complex refractive index (m) of the coating are not known, it is challenging to use α_{abs} to describe the chemical composition of the particles (Gyawali et al., 2009; Lack and Cappa, 2010). In spite the fact that the α_{abs} depends also on the coating, ~~T~~the absorption wavelength dependency is often used to describe the source of the BC (Sandradewi et al., 2008; Zotter et al., 2017). The source apportionment assumes that there are BC emissions only from traffic and wood burning and that the BC from these sources has a specific wavelength dependency.

To investigate how the AOPs at SMEAR II would affect the climate, the aerosol radiative forcing efficiency ($\Delta F\delta^{-1}$ or RFE) was also calculated. The RFE is a simplified formula that describes how large a difference the aerosol particles would make to the radiative forcing (ΔF) per unit of aerosol optical depth (δ) (Sheridan and Ogren, 1999)

$$\frac{\Delta F}{\delta} = -DS_0T_{at}^2\omega_0\beta(1-A_c)\left[(1-R_s)^2 - \left(\frac{2R_s}{\beta}\right)\left(\frac{1}{\omega_0}-1\right)\right]. \quad (13)$$

RFE does not take into account that the properties and amount of aerosol particles vary vertically in the atmospheric column. In the Eq. ~~11~~13, D is the fractional day length, S_0 the solar constant, T_{at} the atmospheric transmission, A_C the fractional cloud amount, and R_S the surface reflectance for which the following constants were used respectively: D = 0.5, S_0 = 1370 Wm^{-2}, T_{at} = 0.76, A_C = 0.6 and R_S = 0.15. The values were according to Haywood and Shine (1995), who used these values independent of wavelength in calculating the ΔF. Sheridan and Ogren (1999) used these same constants later in calculating the RFE at 550 nm. In this study we determine the RFE at 550 nm. The factor β is the upscatter fraction and is calculated using b (Delene and Ogren, 2002)

$$\beta = 0.0817 + 1.8495b - 2.9682b^2. \quad (14)$$

It must be noted that Eq. 14 does not take into account the variation in the sun's zenith angle.

As stated by Sherman et al. (2015), the purpose of determining the RFE is to provide a means for comparing the intrinsic aerosol forcing efficiency of aerosols measured at different sites. We calculated the RFE by using the constant values to have results comparable with other studies in very different types of environments (e.g. Sheridan and Ogren, 1999; Andrews et al., 2011; Sherman et al., 2015; Shen et al., 2018) and to study how the RFE changes with varying ω_0 and b. Here we refer the RFE that was calculated by using the above-mentioned constant values as $RFE_{H\&S}$. It must be noted that ω_0 and b used in Eq. 13 are defined for dried sample air; thus $RFE_{H\&S}$ does not represent ambient air. In the ambient air, RH is larger and the AOPs change due to hygroscopic growth.

In addition to $RFE_{H\&S}$, we calculated a seasonal RFE by allowing the D to vary and by using more realistic seasonal values for A_C, and R_S. The seasonal variations of these parameters are presented in Fig. S1. Here we refer the seasonal RFE as RFE_S. The effect of ambient RH on ω_0 and b, and hence to RFE, was also studied. The seasonal RFE calculated for ambient RH is referred as $RFE_{S,moist}$. More information about the seasonal D, A_C, R_S, and RH can be found in the supplementary material Sect. S2.

Seasonal A_C was derived by using a ceilometer data. The ceilometer was deployed at the Halli airport (about 25 km from SMEAR II) by Finnish Meteorological Institute (FMI) in 2010. The data were averaged for each month to get a seasonal variation. The lowest mean A_C was in July (~0.25) and the highest in January (~0.76).

For the seasonal R_S, reflectivity determined by Kuusinen et al. (2012) was used. They determined the R_S in a boreal forest for different amounts of canopy snow cover. According to the FMI, the average season of snow cover in Hyytiälä is from 16

November to 20 April (FMI: http://ilmatieteenlaitos.fi/lumitilastot, in Finnish only, last accessed: 13 March 2019) and for that time period we used $R_S = 0.314 \pm 0.14$ that Kuusinen et al. (2012) determined as the average albedo for a snow covered canopy. For snow-free forest we used $R_S = 0.126$, which is an average of the mean monthly albedos Kuusinen et al. (2012) determined for snow-free months.

In calculating the ω_0 for ambient air, we used the equations (Eqs. 1 and 2) and parametrization presented in Sect. 2.3.1 to convert the σ_{sca} for ambient RH; σ_{abs} was assumed to be constant with increasing RH, as Nessler et al. (2005) showed that the change in the σ_{abs} with increasing RH is very small compared to scattering. There has not been measurements of hygroscopic growth parameters (q and γ) for σ_{bsca}, so we could not use the same parametrization in calculating the b to ambient RH. Fierz-Schmidhauser et al. (2010) observed about 30 % decrease in b when the RH increased to 85 % at the Jungfraujoch measurement station. We used this observation as a linear approximation to estimate the how the b changes with varying RH. The estimated b was then used in calculating the β for moist conditions. The seasonally averaged RH was determined from RH measurements conducted at the height of 16 m. The lowest mean RH occurred in May (~62 %) and the highest in November (~95 %).

The estimated uncertainties for the intensive AOPs are presented in Sect. S3 in the supplementary material. The uncertainties were calculated according to Sherman et al. (2015).

2.3.4 Data coverage

If averaged over the whole measurement period, 81 % of the nephelometer data and 70 % of the aethalometer data were considered valid. All the AOPs had some gaps in the data (see Fig. 1). Monthly data coverage of σ_{sca} and σ_{abs} are presented in Table S1. Most of the gaps in the time series of AOPs during the summers of 2006 to 2010 were due to too high RH. The gap in 2010 was due to maintenance and installation of the dryers and the switching inlet system. Some additional σ_{bsca} data were missing, due to malfunction of the backscatter shutter of the integrating nephelometer. Dirty optics, malfunctions and maintenance caused the gaps in the σ_{abs} data in 2012 and 2015.

Until March 2010, the integrating nephelometer and the aethalometer measured sample air that was not dried with any external dryers. During winter, the relative humidity (RH) remained below 40 %, since the sample air warmed up to room temperature (about 22 °C). Sometimes in summer, the RH of the sample increased to over the 40 % limit. If the RH was above 40 %, the data were flagged as invalid and they were omitted from the data analysis if not stated otherwise. About 25 % of all the data before March 2010 had to be removed due to too high RH. Almost all of the removed data was from summer and fall months (June – October) and if regarding only these months, 46 % of the data were flagged. If the moist data was included the overall data coverage would increase to 89 % and 77 % for scattering and absorption data, respectively. After the installation of the Nafion-dryers in March 2010, the humidity caused no further problems.

2.4 Properties calculated from particle size distributions

With the size distributions it is possible to calculate differently weighted mean diameters. In this study, we used the geometric mean diameter (GMD) and the volume mean diameter (VMD). The GMD is the mean diameter that is weighted by the number concentration (N)

$$\mathrm{GMD} = \exp\left(\frac{\sum N_i \ln D_{p,i}}{\sum N_i}\right), \quad (15)$$

while the VMD is weighted by the particle volume (V)

$$\mathrm{VMD} = \frac{\sum D_{p,i} V_i}{V_{tot}} = \frac{\sum N_i D_{\mathrm{p},i}^4}{\sum N_i D_{\mathrm{p},i}^3}. \quad (16)$$

Since the number concentration is focused on the nucleation and Aitken mode particles, the GMD describes the distribution changes in the smallest sizes. The VMD, in contrast, is affected by the changes in the accumulation and coarse mode, since they contribute the most to the volume size distribution.

The measurements of the AOPs and size distribution can be combined by determining the complex refractive index ($m = n + ik$) that describes how much the particles scatter and absorb light and can be used to model σ_{sca}, σ_{bsca} and σ_{abs} from the size distribution measurements. Index m consists of the real part (n), which accounts for the scattering, while the absorption is described by the imaginary part (k). Like ω_0, m provides information on the darkness and the chemical composition of the aerosol particles.

In this study, m was iterated from the σ_{sca}, σ_{abs} and size distribution measurements in a manner similar to that described by Virkkula et al. (2011). In the first step of the interpolation $\sigma_{sca,Mie}$ and $\sigma_{abs,Mie}$ were determined for the measured size distribution by using the Mie-theory with initial $m = 1.544 + 0.019i$. The calculated $\sigma_{sca,Mie}$ and $\sigma_{abs,Mie}$ were then compared with the measured σ_{sca} and σ_{abs}. If the calculated and measured values did not agree the real part of m was first varied stepwise by 0.001 until the measured and modeled σ_{sca} agreed. Next, the imaginary part of m was varied in the same way until the measured and modeled σ_{abs} agreed. This iteration was continued until the measured and calculated values agreed within 1 %. The new imaginary part of m also affected σ_{sca} so the real part had to be reiterated. ~~This iteration was continued until the measured and calculated values agreed within 1 %.~~ The MATLAB codes developed by (Mätzler, 2002) were used to model the Mie scattering and absorption.

2.5 Trends

The trends and their significance were determined using the seasonal Kendall test described by Gilbert (1987). This test determines if there is a similar trend for each season (month) separately. All of the trends were calculated for the monthly medians, and at least 14 days of valid data in a given month were required for this month to be taken into account in the trend analysis.

3 Results and discussion

Below we first present the descriptive statistics of the AOPs, their trends, and seasonal variations at SMEAR II. The figures of the AOPs in this section are presented in the green wavelength (550 nm for the scattering and intensive properties and 520 nm for the absorption measurements). In the figures of α_{sca} and α_{abs}, wavelength ranges of 450–700 nm and 370–950 nm were used. The results are presented for dry aerosols (RH < 40 %) if not stated otherwise.

3.1 Overview of the data

The descriptive statistics of the AOPs of both the PM10 and PM1 particles are shown in Tables 1 and 2, respectively. From Table 1~~Table 1~~ we see that the PM10 AOPs differ somewhat from the results of Virkkula et al. (2011) and Pandolfi et al. (2018) that can be explained by the trends and by differences in the data processing. For example the mean σ_{sca} (~15 Mm^{-1}) at λ = 550 nm in this study was lower than that presented by Virkkula et al. (2011) (~18 Mm^{-1}) and by Pandolfi et al. (2018) (~17 Mm^{-1}), which is probably due to the tendency of σ_{sca} to decrease (see Sect. 4.2). Another reason is that in the data processing Virkkula et al. (2011) used the earlier WMO/GAW recommendation (WMO/GAW, 2003) and used data measured at RH < 50% and did not do any RH corrections. We also determined a strong tendency for σ_{abs} to decrease as well, but the mean σ_{abs} (~2.1 Mm^{-1}, interpolated to 550 nm) was not much lower than the mean (~2.2 Mm^{-1}, at 550 nm) in the study by Virkkula et al. (2011). This was due to the differences in the aethalometer data-processing. Virkkula et al. (2011) reported no flow or spot size corrections and they used the algorithm of Arnott et al. (2005) and C_{ref} = 3.688 at λ = 520 nm. Naturally, the different methods used in the absorption data processing also affected the optical properties that are dependent on the σ_{abs}, such as ω_0 and k. In the correction algorithm by Arnott et al. (2005), the C_{ref} is wavelength depended, which increases the α_{abs}. Virkkula et al. (2011) reported a median α_{abs} = 1.4 that is notably higher than the median α_{abs} = 1.0 determined by our study. The difference in α_{abs} can be attributed to the correction algorithm since also in the present work the average and median α_{abs} = 1.36 and α_{abs} = 1.34 for the wavelength range 370–950 when the Arnott et al. (2005) algorithm is used. (see Table S2).

In comparison to similar studies conducted at other Finnish measurement stations at Pallas in northern Finland (Lihavainen et al., 2015) and at Puijo tower in Kuopio, eastern Finland (Leskinen et al., 2012), SMEAR II showed the highest σ_{sca} and σ_{abs} measured for PM10 particles. At SMEAR II, σ_{sca} was about two times higher and σ_{abs} about three times higher than at Pallas, where the mean values of σ_{sca} = 7.9 Mm^{-1} and σ_{abs} = 0.7 Mm^{-1} were measured at green wavelength. The Pallas station is remote, located 170 km north of the Arctic Circle, far from anthropogenic sources. At SMEAR II, σ_{sca} and σ_{abs} were about 1.~~4~~3 and 1.1 times higher~~, respectively~~, than that measured at the Puijo tower, where the mean values of σ_{sca} = 11.6 Mm^{-1} and σ_{abs} = 1.6 Mm^{-1} were measured at green and red wavelengths, respectively.~~, even though the~~ Puijo tower is a semi-urban measurement station located only 2 km away from the Kuopio city center. At the Puijo tower the measurements were conducted only on particles smaller than 2.5 µm, which explains part of the differences, at least for σ_{sca}.

Even though the σ_{sca} measured at SMEAR II is high compared to other measurements conducted in Finland, the air measured at SMEAR II is still clean when compared to other European stations. Due to the remote location, Pandolfi et al. (2018) observed rather low σ_{sca} at SMEAR II compared to other European sites. Lower median σ_{sca} was observed only in the arctic region, at another Nordic rural station in Birkenes, Norway, and at several high mountain sites~~The mean ω_0 was 0.84 for Puijo tower (at 637 nm), 0.88 for SMEAR II (at 550 nm), and 0.92 for the remote Pallas station (at 550 nm).~~. Highest σ_{sca} Pandolfi et al. (2018) observed in central and Eastern Europe.

The differences between the optical properties of the PM1 and PM10 particles are explained by the differences in concentrations, size distributions and chemical compositions. If only the PM10 data overlapping with the PM1 measurements were taken into account, the median values of σ_{sca}, σ_{abs}, ω_0, b, α_{sca}, α_{abs}, n, and k would have been 9.~~5~~6 Mm^{-1}, 1.3 Mm^{-1}, 0.89, 0.~~15~~14, 1.92, 0.~~96~~97, 1.525 and 0.014 (σ_{sca}, ω_0, b, α_{sca}, n and k at 550 nm, σ_{abs} at 520 nm), respectively. The extensive variables (σ_{sca}, σ_{bsca} and σ_{abs}) were smaller for the PM1 measurements, since there was less particle volume interacting with the radiation. Due to the differences in the median ω_0 and n, the PM1 particles absorbed more light relative to scattering than the PM10 particles. The α_{sca} and b are related to the sizes of the particles, so they were naturally different between the PM1 and PM10 particles. For the smaller PM1 particles, the α_{sca} and b were larger than for the PM10 particles. However, b does not have as large a difference between the PM1 and PM10 particles as α_{sca}.

The average values of the PM10 particles given in Table 1 are calculated by excluding the periods when the RH > 40 %. If these periods of σ_{sca} and σ_{abs} measurements were included in the analysis and the moist scattering data were corrected to dry conditions by using the Eqs. 1 and 2, we would get median values of σ_{sca} = 10.3 Mm^{-1}, σ_{abs} = 1.5 Mm^{-1}, ω_0 = 0.88, b = 0.15, α_{sca} = 1.91, α_{abs} = 0.98, and RFE$_{H\&S}$ = -23 for PM10 (σ_{sca}, ω_0, b, and RFE$_{H\&S}$ at 550 nm, σ_{abs} at 520 nm, α_{abs} at 370 nm/950 nm and α_{sca} at 450 nm/700 nm). The differences are not large compared to values presented in Table 1, so omitting the moist data periods from the data set does not seem to have a large effect on the median AOPs in this data set.

3.2 Trends

The long time series of the PM10 and PM1 AOPs were used to determine the trends for the optical properties. For the PM10 trend analysis we used data from about 10.5 years and for the PM1 trend analysis we used about 7.5 years long time series. The slopes of the trends and the trend statistics are presented in Table 3. The table also presents the trends as percentages, which were calculated by dividing the slope by the overall median value of the variable. The trends are also plotted in Fig. 1, where the monthly medians of the PM10 AOPs at SMEAR II used in this analysis are presented. The monthly medians are included in Fig. 1~~Fig. 1~~ only if the month had at least 14 days of valid data.

In the extensive properties, the trends were negative. The slopes of the trends for PM10 σ_{sca}, σ_{bsca} and σ_{abs} were -0.32, -0.038, and -0.~~088~~ 086 $Mm^{-1}yr^{-1}$, respectively. The decrease in the extensive properties were due to decrease in the total particle number concentration (N_{tot}) and total volume of the particles (V_{tot}) that can be seen in the combined TDMPS and APS data presented in Figs. 2a and b~~Figs. 2a and b~~ and in Table 3. The relative decrease in V_{tot} (-4 $\%yr^{-1}$) was rather similar to that of σ_{sca} (-3 $\%yr^{-1}$). Also, Pandolfi et al. (2018) showed a statistically significant trend for σ_{sca} (-0.588 $Mm^{-1}yr^{-1}$) measured at SMEAR II. They reported negative trends at other European sites as well and they determined that the average decrease was about -35 % for a ten-year period, which is a bit larger reduction than that observed at SMEAR II (-30 % for a ten-year period). The results are in line with the decrease in particle number concentration observed in European countries (Asmi et al., 2013). Also the remotely measured decreasing trend for aerosol optical depth (δ) supports the decreasing trends in Europe (Li et al., 2014). Decreasing trends for σ_{sca} are not only observed in Europe; Collaud Coen et al. (2013) and Sherman et al. (2015) reported negative trends for σ_{sca} in North America as well.

The observed relative decrease in σ_{abs} (-6 $\%yr^{-1}$) was about twice as large than that of σ_{sca} (-3 $\%yr^{-1}$). The differences in the trends indicates that during the measurement period, the amount of absorbing material, such as BC and BrC, decreased relatively faster than the amount of scattering material (e.g. sulfate). It is also possible that the decrease in non-absorbing compounds decreased the σ_{abs} since a non-absorbing coating around an absorbing particle can act as a lens, which increases absorption. The study by Collaud Coen et al. (2013), which included also σ_{abs} data, observed negative trends for both σ_{sca} and σ_{abs} at the Bondville measurement station in Illinois, USA. There the trends of σ_{sca} and σ_{abs} were similar in magnitude (about -3 % yr^{-1}). Sherman et al. (2015) did not observe this decreasing σ_{abs} trend later.

For the PM1 σ_{abs}, we observed a very steep decrease (-12 % yr^{-1}), which was probably caused by very high σ_{abs} measured in January and February in 2012. Also, the data gaps in winter 2013 and 2015 could have affected the trends. The time series, of which the trends were determined for the PM1 measurements, were only 7.5 years long. Trends, which are determined for shorter time series, are more sensitive to year-to-year variability. This kind of extreme values can induce relatively large trends, which is why trend analysis for short time series (less than ten years) should be treated with caution.

Since the aerosol particles were absorbing less light than before, there was a tendency for the ω_0 to increase. As shown by the increase in ω_0 and the decrease in the extensive properties, the air measured at SMEAR II was less polluted than before. The higher ω_0 indicates that the measurements were less affected by particles produced by traffic emissions or incomplete combustion. Li et al. (2014) reported mostly positive trends that were determined by remote measurements conducted in Europe. The decreasing trend for k supports the tendency for ω_0 to increase, since the negative trend for the imaginary part of m means that particles absorb less light. The α_{abs}, which is also related to the chemical composition of the particles, showed no significant trend for either the PM1 or PM10 particles. The negative trend for the interpolated n was only significant for the PM1 particles. The tendency for the interpolated n to decrease could have been caused by changes in the chemical composition.

The trends of the b and α_{sca} were also investigated. These trends describe how the size distribution of the aerosol particles has changed. For the PM10 b and α_{sca} the trends were positive, but for the PM10 α_{sca} however, the p value was 0.07 so there was only a weak evidence for the positive trend in PM10 α_{sca}. For the PM1 the trends for both, b and α_{sca}, were positive and statistically significant. Increasing b and α_{sca} indicates that the mean size of the size distribution was moving towards smaller particles. The shift of in the size distribution towards smaller diameters is also observed in the negative trend of the volume mean diameter (VMD_{tot}), presented in Fig. 2c and in Table 3, supporting the increase in b and α_{sca}.

Also, Pandolfi et al. (2018) observed increasing trends for b at SMEAR II and other European stations. For the α_{sca}, however, they observed both positive and negative trends at different stations. Pandolfi et al. (2018) suspected that the variation was caused by differing trends of the coarse and accumulation mode particle concentration. Li et al. (2014) observed negative trends for the α_{sca} across the Europe and they suggested the trends were caused by a decrease in fine particle emissions.

Since the trends of b and α_{sca} for the PM10 and PM1 measurements were similar, the trends in α_{sca} and b may indicate that the concentration of larger particles in the accumulation mode was decreasing, since a decrease in coarse particle concentration only could not cause the decreasing trend of PM1 α_{sca}. The changes in the size distribution were investigated by determining a trend for each TDMPS and APS measurement channels. The results, which are presented in Fig. S4, pointed out that relatively greatest decrease occurred for accumulation mode particles that were 500 – 800 nm in diameter. On average, the volume size distribution of accumulation mode particles peaks around 300 nm (see Figs. S6 and S7) so the greatest decrease occurred at the larger sizes of the accumulation mode. The decrease in this size range might be caused by decrease in long-range transported pollution. Aged pollution particles might be grown by other substances, such as SO_2 in the atmosphere so their sizes are larger than freshly emitted or formed particles. SO_2 emissions have decreased in Europe (Tørseth et al., 2012), which supports this assumption. A trajectory analysis by Virkkula et al. (2011) showed that α_{sca} was clearly higher in air masses from continental Europe than from the North Atlantic and but also that the highest α_{sca} values were measured in air masses sources from within southern Finland, which would suggest that larger particles are not from nearby the station.

The installation of the Nafion-dryers in 2010 could have caused an artificial decrease in σ_{sca} or σ_{abs} since the dryers increase the deposition of the particles and may decrease the sizes of hygroscopic particles. However, the trends were similar for the PM10 and PM1 particles. During the PM1 measurements, there were no large changes in the measurement line, so the observed trends were probably not caused by any technical changes in the measurement line.

A lot of summer time data measured before 2010, were marked invalid due to too high humidity and it could have affected the trend analysis. To test this hypothesis, we used Eqs. 1 and 2 to correct the σ_{sca} to dry conditions and included this data in the trend analysis. The σ_{bsca} was not corrected to dry conditions. Also, moist (RH > 40 %) absorption data was included in this test. Including the originally omitted data in the trend analysis, we observed statistically significant (p-value < 0.05) trends for the PM10 σ_{sca}, σ_{abs}, ω_0, and RFE with the slopes of -4 % yr^{-1}, -5 % yr^{-1}, 0.2 % yr^{-1}, and 0.5 % yr^{-1} respectively. Still, there were decreasing trends for extensive properties and positive trends for ω_0. However the difference between the σ_{sca} and σ_{abs} trends decreased from 3 % to 1 % if compared against the trends that were determined only for the dry conditions. Including the moist data and acquiring longer data sets in the trend analysis suggests that the relative difference between the trends of σ_{sca} and σ_{abs} might not be that large. Not correcting the σ_{bsca} to dry conditions probably explains why we do not see a significant trend for the b here.

In addition to the general trends, we also investigated how the trends of σ_{sca} and σ_{abs} varied between different seasons. In this analysis, the periods of RH > 40 % were included (σ_{sca} corrected to dry conditions according to Eqs. 1 and 2) in order to avoid the data gaps in summer and autumn before 2010. The trends were determined separately for spring (March, April, May), summer (June, July, August), autumn (September, October, November), and winter (December, January, February). The trend calculations were conducted by using the monthly medians (see timeseries in Fig. S3). The results are presented in Table 4.

Table 4 shows that σ_{sca} and σ_{abs} had a decreasing trend for each season, but for the autumn the trends were not significant. Both σ_{sca} and σ_{abs} experience the fastest absolute decrease in winter when the energy consumption is the highest and pollution sources are more pronounced; on the opposite, the trends are the least negative in summer. In spring, the absolute trends were less negative than compared to winter. However, for the σ_{abs} we observed that the relative trend in spring (-9 %yr^{-1}) was steeper than in winter (-8 %yr^{-1}).

3.3 Aerosol optical properties and size distribution

To obtain a better view on how the shape of the size distribution affected the AOPs, the various AOPs were compared against the GMD and VMD. The results of the comparison are shown in Fig. 3. The GMD was mostly affected by the small nucleation

and Aitken mode particles, which are high in number concentration; the accumulation mode particles also had some effect on the GMD. Since only the smallest particles affect the GMD it is practically the same for the fine (D_p < 1 µm) and total (D_p < 10 µm) particle size distribution. Thus we present the comparison of GMD and AOPs only for the PM10 particles (Figs. 3a – d). The VMD, however, was heavily affected by the size distribution of the accumulation and coarse mode particles, since they predominated in the particle volume size distribution. This explains why there was notable differences for the PM10 (Figs. 3e – h) and PM1 (Figs. 3i – l) particles, when their AOPs were compared against the VMD calculated for particles smaller than 10 µm (VMD_{tot}) and VMD calculated for particles smaller than 1 µm (VMD_{fine}), respectively.

The σ_{sca} correlated positively with the GMD due to the changes in particle concentration in the accumulation mode. The median number and volume size distribution for situations when GMD was below 50 nm or above 100 nm are presented in Fig. 4c. There was a clear difference in the number and volume size distribution in the accumulation mode when the GMD limit was varied. From the number size distribution, it can be seen that GMD increased due to a larger accumulation mode and lack of particles in the nucleation and Aitken modes. Nucleation and Aitken mode particles are mainly produced and grown by condensing vapors and since larger particles in the accumulation mode act as a condensation sink for vapors, the smaller particle modes do not tend to exist when accumulation mode particles are present.

For the PM10 particles, there was a negative correlation between the σ_{sca} and VMD, but when the coarse particles were ignored, i.e. for PM1 particles the correlation became positive. The negative correlation for the PM10 particles is caused by the changes in the accumulation and coarse mode particle concentration. This is shown in further detail in Fig. 4a, where the median volume size distribution is presented for situations in which the VMD_{tot} > 1500 nm, 500 nm < VMD_{tot} < 1000 nm and VMD_{tot} < 500 nm. When the VMD_{tot} was high, there was a strong coarse mode but the accumulation mode was clearly smaller than in the other situations. Even though the VMD_{tot} was high, the lack of accumulation mode particles decreased the scattering. From Fig. 3a~~Fig. 4a~~, it can be seen that the σ_{sca} became maximal when the VMD_{tot} was about 500–1000 nm. In this VMD range, the coarse mode was slightly smaller but the accumulation mode clearly increased, thus increasing the scattering. When the VMD_{tot} < 500 nm, the coarse mode was almost completely missing that caused the σ_{sca} to decrease, even though there was a large accumulation mode present.

Kulmala et al. (2016) estimated that fresh eBC particles observed at SMEAR II are in the size range of 80 – 120 nm. That estimate was calculated in a simplified way from the relationship between particle number concentrations and BCe concentrations. A better estimate is obtained from the size dependence of ω_o. The darkest aerosol has ω_o < 0.6 and GMD in the range of about 30 – 70 nm (Fig. 3b, 3f, and 3j). This has been shown to be the range of fresh BC (e.g., Kittelson, 1998; Casati et al., 2007; Zhang et al., 2008) which suggests the source of BC is not far, probably within some kilometers only.

The size-dependent properties α_{sca} and b for PM10 acted rather differently when compared with the GMD and VMD_{tot}. The~~When the GMD was higher, the~~ α_{sca} ~~also~~ increased with growing GMD (Fig. 3c), which ~~that~~ is in contrast with the expectation that the α_{sca} would decrease when the size distribution is dominated by larger particles. The observation that the α_{sca} increased with an increasing GMD is in line with the analyses made for AOPs and size distributions measured in Guangzhou, China by Garland et al. (2008), at SMEAR II by Virkkula et al. (2011), and in Nanjing, China by Shen et al. (2018). To study the reasons behind this relationship we generated first unimodal size distributions with two geometric standard deviations GSD = 1.5 and 2.0 and calculated both σ_{sca} and σ_{bsca} at λ = 450, 550, and 700 nm with the Mie code with m = 1.517 + 0.19i and the α_{sca} and b from them. For unimodal size distributions the α_{sca} decrease~~d~~ with increasing GMD~~,~~ as is shown by the lines in Fig. 3c. ~~They were calculated by generating unimodal size distributions with the geometric standard deviations GSDs = 1.5 and 2.0 and calculating the σ_{sca} for λ = 450, 550, and 700 nm with the Mie code with m = 1.517 + 0.19i and the α_{sca} from them.~~ Schuster et al. (2006) showed that the relationship may be the opposite for ~~a~~ bimodal size distribution~~s~~. Schuster et al. (2006) explained this behavior by that adding a larger or coarse particle size mode to a fine particle mode that is inefficiently scattering - for instance nucleation and Aitken mode particles – the larger mode contributes more efficiently to the Ångström exponent than the fine mode. The contribution of the particles smaller than 100 nm to GMD is larger than that of the larger particle modes which leads to the observed relationship. To study this in more detail we generated also bimodal size distributions. The analysis presented in the supplement (S6) shows that the α_{sca} of bimodal size distributions can be calculated as a linear combination of the α_{sca} of the modes, weighted by the fractions of σ_{sca} of the respective modes. This explains the increase of α_{sca} with growing GMD.

In addition, ~~A~~at SMEAR II the size distribution typically consists of not only two but ~~of~~ multiple modes (Dal Maso et al., 2005; Saarikoski et al., 2005) that explains the observed relationship. An additional qualitative analysis of this relationship is given in Fig. 4c, where the median number and volume size distributions are plotted for situations in which the GMD was < 50 nm and > 100 nm. By comparing these two situations, it can be seen that when the GMD > 100 nm the accumulation mode was much larger than when GMD < 50 nm. Since the coarse mode is rather similar for both cases, the α_{sca} varied due to changes in the accumulation mode. For the α_{sca} and VMD, the correlation was negative (Fig. 3g) that supports the expectations. However, the α_{sca} measured for the PM10 particles was much higher than that modeled for the unimodal distributions, which can also be explained by the multiple modes of the real size distributions.

There was a negative correlation between the GMD and PM10 b (Fig. 3d) as expected, but the correlation was rather weak. On the contrary, the correlation between the VMD_{tot} and PM10 ~~α_{sca}~~ b was slightly positive (Fig. 3h). The ~~positive~~ negative correlation of α_{sca} with VMD_{tot} and the ~~negative~~ positive correlation of b with VMD_{tot} for the PM10 particles indicates that the

α_{sca} and b were sensitive to different size ranges. The α_{sca} decreased when there are more coarse particles present, but for the b the coarse particles seem to have no expected effect and the b increased with increasing VMD_{tot}. Fig. 4a. shows that when the VMD > 1500 nm, the peak of $DV/d\log D_p$ in the accumulation mode was much lower and tilted towards the smaller diameters than compared to the situations where the VMD < 1000 nm. This is in line with Collaud Coen et al. (2007), who stated that in the Jungfraujoch data, b was sensitive to particles smaller than 400 nm and that the sensitivity of the α_{sca} was at its maxima for particle diameters between 500 and 800 nm.

For the PM1 particles, the measured α_{sca} and b were well in line with the modeled values (Figs. 3k and l), since the coarse mode particles were removed prior to the measurements, the shape of the size distribution was closer to a unimodal size distribution, and the VMD_{fine} described better how the accumulation mode shifted.

3.4 Seasonal variation

The seasonal variation in the PM10 AOPs was clearly visible in the 12-year record shown in Fig. 5. The seasonal variation in σ_{sca} and σ_{bsca} (Figs. 5a and b) was not yet as clear in Virkkula et al. (2011) as it is now. For the σ_{sca} and σ_{bsca}, two local maxima occurred during late winter (February) and late summer (July). The local minima occur during spring (April) and late autumn (October). The σ_{abs} showed the highest values during winter (February) and the lowest values during summer (June). Part of this variation is explained by boundary layer dynamics. In summer, the boundary layer is higher and well mixed thus diluting the aerosol concentration. In winter the situation is the opposite and the pollution accumulates in the shallow boundary layer.

For the extensive properties, the highest values occurred at the same time in winter (February) when the ω_0 was also low, which means that there were larger amounts of particles from anthropogenic sources than in summer. Hyvärinen et al. (2011) observed increased equivalent eBC concentrations at SMEAR II in winter, when the long-range transport brings pollution from the central and eastern Europe. However, Hienola et al. (2013) estimated that about 70 % of the measured eBC at SMEAR II is emitted from local or regional sources or transported from Finnish cities so also the local and regional emissions have a significant role in the elevated eBC concentrations. Since February is one of the coldest months in Finland, domestic wood burning in the local and regional area increases the particle concentration (Karvosenoja et al., 2011). Pollution can also be transported from nearby cities (the largest and closest are Tampere and Jyväskylä). Hyvärinen et al. (2011) observed no remarkable changes in the Hyytiälä eBC concentrations coming from the Tampere region. However, the largest concentrations they observed came from the direction of Orivesi, a small town (population about 9 000) 20 km from the measurement station.

In summer, the ω_0 had its highest values since the σ_{sca} was high and the σ_{abs} was low. In summer, the anthropogenic influence is not as strong as in the winter since the energy consumption is lower. The contribution of particles from natural sources

increased during spring and summer when the vegetation was active and growing. The seasonal variation in the n and k was clearly associated with the ω_0. In summer when the ω_0 was high, n was high and k was low. In winter, the relationship was the opposite. The scattering maximum in summer was probably caused by secondary organic particles (Tunved et al., 2006) explaining why the b and α_{sca} are also maximal.

There is an anti-correlation between the seasonal variations of ω_0 and α_{abs}. The maximum values of α_{abs} (> 1) occur in winter, which means that light is absorbed more efficiently at shorter wavelengths than in summer. A higher α_{abs} may suggest that light is absorbed not only by BC, but also by some light-absorbing organic carbon compounds, i.e. brown carbon (BrC). In using only α_{abs}, it is difficult to determine if the particles consist of BrC, since BC particles with coating can also have an α_{abs} up to 1.6 (Lack and Cappa, 2010). In Fig. 5 we can see that the value of 1.6 is not really reached at SMEAR II. Since α_{abs} is dependent on the size of the BC core, the thickness of the coating and the m of the coating, more detailed investigation would be needed to determine why α_{abs} is varies.

Also, the α_{abs} is typically associated with the source of the BC and it is often used to quantify whether the BC is traffic or wood burning related (Sandradewi et al., 2008; Zotter et al., 2017) so that high α_{abs} is a sign of wood burning. In the source apportionment, α_{abs} close to one indicates that the BC is sourced from traffic. Since we observed relatively higher α_{abs} in winter, the results are in line with the assumption of domestic wood burning that takes place during winter. However, in summer, α_{abs} was often < 1, which would yield an unphysical fraction (over a 100 %) of traffic related BC. Values below 1 could have been caused by large BC particles (D_p > 100 nm) that have a purely scattering coating (Lack and Cappa, 2010). It must be noted that the α_{abs} depends also on the correction algorithm. For example, if the σ_{abs} was corrected with the algorithm proposed by Arnott et al. (2005), the mean ± SD of α_{abs} would have been 1.36 ± 0.51 (see Table S2). Using the α_{abs}, which was determined by using the correction by Arnott et al. (2005), the results for the source apportionment would be different and they would show higher fraction of BC from wood burning. Further investigation of the complex nature of α_{abs} is omitted here.

The seasonal variation in α_{sca} and b depends on the seasonal variation in the size distribution of the particles. Both α_{sca} and b were maximal in summer and minimal in winter, suggesting that in summer, the particle population consisted of smaller particles than in winter. Closer investigation on the size distribution, which is presented in Fig. S6 and S7, reveals that in winter, the VMD_{tot} was experiencing it minimum due to a lack of coarse mode particles. This is in contrast with the observation or smaller α_{sca} and b. In fact, the seasonal variation of α_{sca} and b was explained by the seasonal variation of accumulation mode and VMD_{fine}, which is a good indicator for the shifting accumulation mode. In winter, the accumulation mode was shifted towards larger sizes and the median of VMD_{fine} was about 350 nm. In summer the situation was the opposite and VMD_{fine} was about 250 nm.

3.5 Variation between the PM10 and PM1 measurements

Even though the average values between the optical properties of the PM10 and PM1 particles differed, their seasonal variation was similar for all the various properties. However, there was a seasonal variation in the relationship between the PM10 and PM1 extensive properties, as shown in Fig. 6. The seasonal variation in the PM1/PM10 ratio describes the impact of the coarse and fine particles on the σ_{sca} and σ_{abs}.

For the σ_{sca} the seasonal variation in the PM1/PM10 ratio was clear, but for the σ_{abs} there seemed to be no seasonal variation in the ratio whatsoever. The seasonal medians of the PM1/PM10 ration for the σ_{sca} varied from 0.7 to 0.8, and on average submicron particles caused about 75 % of the total scattering of the PM10 particles. This was apparently a lower fraction than in the previous analysis of SMEAR II scattering data. Virkkula et al. (2011) stated that the seasonal average contributions of submicron particles to the total σ_{sca} was in the range of 88–92 %, clearly more than in the present work. However, in that study the scattering size distribution and the contributions of the various size ranges were calculated from particle number size distributions with a Mie model and the physical diameters (D_p) were used whereas here the PM1 corresponds to particles smaller than the aerodynamic diameter D_a of 1 µm. With particle density of 1.7 g cm^{-3} this corresponds to the physical diameter $D_p = (1/1.7)^{½}$ 1 µm ≈ 0.77 µm. The contribution of particles smaller than 0.77 µm is approximately 85 % if it is estimated from Fig. 11 of Virkkula et al. (2011), still more than the ~75 % contribution of submicron scattering shown here. This may have resulted from the cutoff diameter of the PM1 impactor is not exactly sharp and also that the particles entering the impactor may have still been somewhat moist and thus larger than their dry size and were therefore removed from the sample stream. Further analysis of the difference is omitted here.

The maxima of the submicron particle scattering occurred in winter and summer. The summer peak coincided with the maxima of the PM10 α_{sca}, which already indicates that smaller particles play a major role in the size distribution. However, this correlation between the PM1/PM10 ratio and α_{sca} was not observed in winter. In Fig. 2~~Fig. 2~~ (and in Fig. S7), it can be seen that the VMD_{tot} always decreased in the wintertime indicating also the lack of coarse particles. However, on average, the accumulation mode is relatively large compared to the coarse mode and it is shifted towards the larger diameters. This is presented in the supplementary material (Figs. S6 and S7). The large accumulation mode caused α_{sca} to be low, even though there was relatively less scattering by the coarse particles.

For the σ_{abs}, the median of the PM1/PM10 ratio did not greatly vary seasonally. The PM1 particles absorbed about 90 % of the total PM10 particle absorption. So for the σ_{abs} there were no large difference in the σ_{abs} of the PM1 and PM10 particles. The coarse mode particles are typically primary and they have a quite high ω_0 so their absorption is minor compared with the PM1 particles. The soot particles, which account for most of the particulate absorption, are typically submicron particles.

The deviation of the σ_{abs} PM1/PM10 ratio clearly varied seasonally. In summer, the variation was considerably higher than in winter. In the correction algorithm, which was used for the absorption data (Eq. 3), part of the σ_{sca} is subtracted from σ_{abs} as an apparent absorption (Muller et al., 2011). This subtraction causes relatively high uncertainty when the σ_{abs} is low and σ_{sca} is high like it is in summer. This uncertainty is emphasized for PM10 measurements, since the σ_{sca} is relatively higher than σ_{abs} if compared to PM1 measurements. The uncertainty in the measurements also explains why there were so many values above 1 measured in the PM1/PM10 σ_{abs} ratio.

The evolution of the PM1/PM10 ratios were also investigated but we observed no statistically significant trends for either σ_{sca} or σ_{abs}.

3.6 Radiative forcing efficiency

For the aerosol radiative forcing efficiency (RFE) the mean values, trends, and seasonal variation were also investigated. The statistics of the $RFE_{H\&S}$, RFE_S and $RFE_{S,moist}$ are presented in Table 1 and their time series and seasonal variation are presented in Figs. ~~7a and b~~7.

In general, the aerosols, measured at SMEAR II, tend to have a cooling effect on the climate (RFE < 0) as seen in Table 1. By using the global average values suggested by Haywood and Shine (1995), the mean $RFE_{H\&S}$ was -22 Wm^{-2}. This is about 12 % less negative than the mean $RFE_{H\&S}$ (about -25 Wm^{-2}) determined by Sherman et al. (2015) for different North American stations. The difference is explained by higher mean ω_0 (about 0.91) observed by Sherman et al. (2015), the mean b (about 0.14) was similar if compared to average values observed at SMEAR II. Also, a mean $RFE_{H\&S}$ -25 Wm^{-2} was determined at SORPES in China (Shen et al., 2018). Shen et al. (2018) observed a notably higher mean ω_0 (0.93 at 520 nm) than what we observed at SMEAR II (0.87), but for the b the situation was the opposite and it was lower at SORPES (0.12 at 525 nm) than at SMEAR II (0.14 at 550 nm). This would suggest that for dry particles the variation of ω_0 is more pronounced than the variation of b in context of calculating the $RFE_{H\&S}$. This is also observed at SMEAR II (Fig. S9). If the seasonal variation of D, A_C, and R_S were taken into account, the mean RFE_S (-34 Wm^{-2}) was more negative than $RFE_{H\&S}$.

Both, the ω_0 and b tended to increase, which makes the $RFE_{H\&S}$ to decrease (i.e., become more negative). The decreasing $RFE_{H\&S}$ means that the properties of dry aerosol particles have changed so that they cool the climate more efficiently. The trends for the $RFE_{H\&S}$, RFE_S and $RFE_{S,moist}$ are presented in Table 3 as well. Since we used seasonal averages in calculating the RFE_S and $RFE_{S,moist}$, their trends are also depended only on the changes of the ω_0 and b and thus their trends are also decreasing and similar in magnitude as the trend for $RFE_{H\&S}$. However, in reality the trend of RFE does not depend only on the ω_0 and b. For example, a decrease in the snow cover due to global warming would decrease the R_S and make the decrease of RFE steeper. Here, we omitted further analysis on the effect that the changes of A_C, R_S, T_{at} and RH have on the RFE.

The seasonal variation in the $RFE_{H\&S}$ followed the seasonal cycles of the ω_0 and b. The $RFE_{H\&S}$ was minimal in summer and maximal in winter. Since b was lowest (forward-scattering particles) and the ω_0 is also low (dark particles) in winter, the particles clearly did not have as strong a cooling effect as in summer when particles are smaller and light colored. If the seasonal changes of D, A_C, and R_S, were taken into account, the seasonal variability of RFE_S is amplified remarkably compared to $RFE_{H\&S}$ as seen in Fig. 7b. In winter, the D is lower and the A_C is higher, which are shown in Fig. S1, causing the aerosol particles to have less effect (RFE closer to zero) than in summer. During winter the higher R_S causes the aerosol particles to be less cooling or even warming. We chose to use the R_S determined for a boreal forest according to the surroundings of SMEAR II. However, the area around the station consists also of fields and lakes, which in winter, would act as smooth snow fields. Even for snow containing impurities the R_S is notably higher (> 0.7) than R_s for snow covered boreal forest (Warren and Wiscombe, 1980). Using R_S = 0.7 for winter time data, would increase the RFE_S.

Taking the effect of RH into account increases the ω_0 since the aerosols scatter more light due to hygroscopic growth. However, the same effect decreases the b since the particles grow in size and scatter relatively less light backwards (Birmili et al., 2009). The seasonality of RH is presented in Fig. S1d and on average the RH is higher in winter than in summer. Fig. 7b shows that that the $RFE_{S,moist}$ is less negative in summer compared to RFE_S since the effect of RH on b overcomes the effect on ω_0. Fierz-Schmidhauser et al. (2010) also observed this kind of behavior at the Jungfraujoch station. In winter the situation is the opposite and $RFE_{S,moist}$ is more negative than RFE_S. However, in winter, the effect of RH is small due to the small D and large A_C. In general, the observed effect of the RH on RFE is smaller than the effect of taking the seasonal variation of D, A_C, and R_S into account.

The RFE (or $\Delta F\delta^{-1}$) describes only the efficiency of the aerosol particles in cooling or warming the climate per unit of aerosol optical depth (δ). Eq. 13 assumes that the properties of the aerosol particles are uniform in the atmospheric column that is rarely the case in reality. In ambient air, we should also take into account the variability in RH as a function of height. At the top of the boundary layer we typically have RH values close to 100 %. Here, we determined the RFE by using the RH measured near the ground (16 m). The simplified RFE does not give an absolute value for the aerosol forcing; however, it can still indicate how the changes in AOPs affect the climate.

Even if the RFE was very negative, the influence of aerosol particles on the climate would be small if the δ was small. The δ is highly dependent on the σ_{sca} and σ_{abs}; the more there are scattering and absorbing material in the atmosphere, the higher the δ. This is analyzed in further detail in Fig. 8, where the ω_0 is presented as a function of b. In Fig. 8~~Fig. 12~~ the $RFE_{H\&S}$ is presented with isolines and the σ_{sca} is presented by color-coding. Fig. 8~~Figure 12~~ shows that when the $RFE_{H\&S}$ is most negative, the median σ_{sca} is actually experiencing its lowest value. When the $RFE_{H\&S}$ is closest to zero, the median σ_{sca} is the highest. It

is also seen that when the b is high and the particle size distribution consists of smaller particles, the particles are most efficient at cooling the atmosphere even though the average ω_0 is the lowest.

These relationships were also observed in a study of AOPs at the Station for Observing Regional Processes of the Earth System (SORPES), a measurement station in Nanjing China (Shen et al., 2018). Also, Delene and Ogren (2002) and Sherman et al. (2015) observed similar systematic variability between σ_{sca}, ω_0, b, and $RFE_{H\&S}$ at several North American measurement stations; when the σ_{sca} increases, the ω_0 increases and the b decreases. Sherman et al. (2015) suggested that this variability could be caused by deposition of larger particles, which typically absorb less light. Delene and Ogren (2002) observed that $RFE_{H\&S}$ increases (i.e. becomes less negative) with increasing σ_{sca}, but Sherman et al. (2015) did not observe this trend.

4 Summary and c~~C~~onclusions

In this study, we presented over 11-year long time series of AOPs measured at SMEAR II, a station in southern Finland. With the long time series, it was possible to see statistically significant trends, seasonal variation, and different types of causalities between the optical properties. We compared the AOPs with the aerosol size distribution measurements conducted at the station and observed in detail how the AOPs are dependent on the shape of the size distribution. By comparing the AOPs and size distribution, we were able to determine the m values that can be used in modeling the σ_{sca} and σ_{abs} from size distribution measurements.

The extensive AOPs, as well as the aerosol number and volume concentration, tended to decrease. Our observation was in line with the other studies conducted in Europe and North America that also observed decreasing trends for the extensive AOPs (Collaud Coen et al., 2013; Pandolfi et al., 2018; Sherman et al., 2015), number concentration (Asmi et al., 2013) and aerosol optical depth (Li et al., 2014). This uniform decreasing trend in the amount of aerosol particles suggests that the anthropogenic emissions of particulate matter and gases that take part in secondary aerosol formation has been decreasing in Europe and North America.~~.~~ The observed tendency for b and α_{sca} to increase together with the decreasing extensive properties indicated that the particle size distribution ~~was moving towards~~consisted of less larger particles ~~smaller diameters~~. A more detailed investigation revealed that the number of larger accumulation mode particles decreased relatively the fastest, which also supports the assumed decrease in pollution.

There ~~are~~ were clear~~ly~~ seasonal variations in the AOPs. The largest differences occur during summer and winter. The seasonal variations in the extensive properties ~~and~~, ω_0 and size distribution revealed that in winter the particles have a larger contribution from the anthropogenic sources than during summer.

Since the aerosol particles are smaller and less dark than before, their RFE tended to decrease (i.e. became more negative), which means that the ability of aerosols to cool the climate per unit δ increased. However, since the extensive properties and particle number concentration are decreasing, which means that the δ decreases as well, the total aerosol forcing is probably also decreasing. We determined the RFE to dry aerosol particles by using global average values suggested by Haywood and Shine (1995). To test the sensitivity of RFE to environmental parameters (D, R_S, and A_C), we calculated the RFE also by using more realistic and seasonally averaged environmental parameters. We also determined the RFE for ambient RH, since it is affected by the hygroscopic growth of aerosols. We observed that at SMEAR II the environmental parameters had a higher impact on the RFE than the ambient RH. Here we only studied the effect of AOPs on the RFE. Taking the long-term trend of environmental parameters into account would probably have a large effect on the trend of the RFE.

Data availability

All the data presented in this study is open access. The optical properties and the size distribution data from SMEAR II has been uploaded on the EBAS database (EBAS: http://ebas.nilu.no/, last access: 18 March 2019) run by the Norwegian Institute for Air Research (NILU). Meteorological parameters measured at SMEAR II, such as the RH used here, can be accessed by the Smart-SMEAR online tool (Junninen et al., 2009). Also the Finnish Meteorological Institute provides open access data and we used their online data tool (FMI: https://ilmatieteenlaitos.fi/havaintojen-lataus, last access: 18 March 2019) to access the ceilometer data measured at Halli airport.

References

Aalto, P., Hämeri, K., Becker, E., Weber, R., Salm, J., Mäkelä, J. M., Hoell, C., O'dowd, C. D., Hansson, H.-C., and Väkevä, M.: Physical characterization of aerosol particles during nucleation events, Tellus B: Chemical and Physical Meteorology, 53, 344-358, 2001.

Anderson, T. L., and Ogren, J. A.: Determining aerosol radiative properties using the TSI 3563 integrating nephelometer, Aerosol Science and Technology, 29, 57-69, 1998.

Andrews, E., Ogren, J., Bonasoni, P., Marinoni, A., Cuevas, E., Rodríguez, S., Sun, J. Y., Jaffe, D., Fischer, E., and Baltensperger, U.: Climatology of aerosol radiative properties in the free troposphere, Atmospheric Research, 102, 365-393, 2011.

Arnott, W. P., Hamasha, K., Moosmüller, H., Sheridan, P. J., and Ogren, J. A.: Towards aerosol light-absorption measurements with a 7-wavelength aethalometer: Evaluation with a photoacoustic instrument and 3-wavelength nephelometer, Aerosol Science and Technology, 39, 17-29, 2005.

Asmi, A., Collaud Coen, M., Ogren, J., Andrews, E., Sheridan, P., Jefferson, A., Weingartner, E., Baltensperger, U., Bukowiecki, N., and Lihavainen, H.: Aerosol decadal trends–Part 2: In-situ aerosol particle number concentrations at GAW and ACTRIS stations, Atmospheric Chemistry and Physics, 13, 895-916, 2013.

Backman, J., Schmeisser, L., Virkkula, A., Ogren, J. A., Asmi, E., Starkweather, S., Sharma, S., Eleftheriadis, K., Uttal, T., and Jefferson, A.: On Aethalometer measurement uncertainties and an instrument correction factor for the Arctic, Atmospheric Measurement Techniques, 2017.

Bergin, M. H., Ogren, J. A., Schwartz, S. E., and McInnes, L. M.: Evaporation of ammonium nitrate aerosol in a heated nephelometer: Implications for field measurements, Environmental Science & Technology, 31, 2878-2883, 1997.

Birmili, W., Schwirn, K., Nowak, A., Petäjä, T., Joutsensaari, J., Rose, D., Wiedensohler, A., Hämeri, K., Aalto, P., and Kulmala, M.: Measurements of humidified particle number size distributions in a Finnish boreal forest: derivation of hygroscopic particle growth factors, Boreal Environment Research, 14, 458-480, 2009.

Boucher, O., Randall, D., Artaxo, P., Bretherton, C., Feingold, G., Forster, P., Kerminen, V.-M., Kondo, Y., Liao, H., and Lohmann, U.: Clouds and aerosols, in: Climate Change 2013: the physical science basis. Contribution of Working Group I to the Fifth Assessment Report of the Intergovernmental Panel on Climate Change, Cambridge University Press, 571-657, 2013.

Casati, R., Scheer, V., Vogt, R., and Benter, T.: Measurement of nucleation and soot mode particle emission from a diesel passenger car in real world and laboratory in situ dilution, Atmospheric Environment, 41, 2125-2135, 2007.

Charlson, R. J., Schwartz, S., Hales, J., Cess, R. D., Coakley, J. J., Hansen, J., and Hofmann, D.: Climate forcing by anthropogenic aerosols, Science, 255, 423-430, 1992.

Collaud Coen, M., Weingartner, E., Nyeki, S., Cozic, J., Henning, S., Verheggen, B., Gehrig, R., and Baltensperger, U.: Long-term trend analysis of aerosol variables at the high-alpine site Jungfraujoch, Journal of Geophysical Research: Atmospheres, 112, 2007.

Collaud Coen, M., Weingartner, E., Apituley, A., Ceburnis, D., Fierz-Schmidhauser, R., Flentje, H., Henzing, J., Jennings, S. G., Moerman, M., and Petzold, A.: Minimizing light absorption measurement artifacts of the Aethalometer: evaluation of five correction algorithms, Atmospheric Measurement Techniques, 3, 457-474, 2010.

Collaud Coen, M., Andrews, E., Asmi, A., Baltensperger, U., Bukowiecki, N., Day, D., Fiebig, M., Fjæraa, A. M., Flentje, H., and Hyvärinen, A.: Aerosol decadal trends–Part 1: In-situ optical measurements at GAW and IMPROVE stations, Atmospheric Chemistry and Physics, 13, 869-894, 2013.

Dal Maso, M., Kulmala, M., Riipinen, I., Wagner, R., Hussein, T., Aalto, P. P., and Lehtinen, K. E.: Formation and growth of fresh atmospheric aerosols: eight years of aerosol size distribution data from SMEAR II, Hyytiala, Finland, Boreal Environment Research, 10, 323-336, 2005.

Delene, D. J., and Ogren, J. A.: Variability of aerosol optical properties at four North American surface monitoring sites, Journal of the Atmospheric Sciences, 59, 1135-1150, 2002.

Ehn, M., Thornton, J. A., Kleist, E., Sipilä, M., Junninen, H., Pullinen, I., Springer, M., Rubach, F., Tillmann, R., and Lee, B.: A large source of low-volatility secondary organic aerosol, Nature, 506, 476, 2014.

Fierz-Schmidhauser, R., Zieger, P., Gysel, M., Kammermann, L., DeCarlo, P., Baltensperger, U., and Weingartner, E.: Measured and predicted aerosol light scattering enhancement factors at the high alpine site Jungfraujoch, Atmospheric Chemistry and Physics, 10, 2319-2333, 2010.

Garland, R., Yang, H., Schmid, O., Rose, D., Nowak, A., Achtert, P., Wiedensohler, A., Takegawa, N., Kita, K., and Miyazaki, Y.: Aerosol optical properties in a rural environment near the mega-city Guangzhou, China: implications for regional air pollution, radiative forcing and remote sensing, Atmospheric Chemistry and Physics, 8, 5161-5186, 2008.

Gilbert, R. O.: Statistical methods for environmental pollution monitoring, John Wiley & Sons, 1987.

Gyawali, M., Arnott, W., Lewis, K., and Moosmüller, H.: In situ aerosol optics in Reno, NV, USA during and after the summer 2008 California wildfires and the influence of absorbing and non-absorbing organic coatings on spectral light absorption, Atmospheric Chemistry and Physics, 9, 8007-8015, 2009.

Hari, P., and Kulmala, M.: Station for Measuring Ecosystem–Atmosphere Relations, Boreal Environment Research, 10, 315-322, 2005.

Hari, P., Nikinmaa, E., Pohja, T., Siivola, E., Bäck, J., Vesala, T., and Kulmala, M.: Station for measuring ecosystem-atmosphere relations: SMEAR, in: Physical and Physiological Forest Ecology, Springer, 471-487, 2013.

Haywood, J., and Shine, K.: The effect of anthropogenic sulfate and soot aerosol on the clear sky planetary radiation budget, Geophysical Research Letters, 22, 603-606, 1995.

Haywood, J., and Boucher, O.: Estimates of the direct and indirect radiative forcing due to tropospheric aerosols: A review, Reviews of Geophysics, 38, 513-543, 2000.

Hienola, A., Pietikäinen, J.-P., Jacob, D., Pozdun, R., Petäjä, T., Hyvärinen, A.-P., Sogacheva, L., Kerminen, V.-M., Kulmala, M., and Laaksonen, A.: Black carbon concentration and deposition estimations in Finland by the regional aerosol-climate model REMO-HAM, Atmospheric Chemistry and Physics, 13, 4033, 2013.

Hyvärinen, A.-P., Kolmonen, P., Kerminen, V.-M., Virkkula, A., Leskinen, A., Komppula, M., Hatakka, J., Burkhart, J., Stohl, A., and Aalto, P.: Aerosol black carbon at five background measurement sites over Finland, a gateway to the Arctic, Atmospheric Environment, 45, 4042-4050, 2011.

Junninen, H., Lauri, A., Keronen, P., Aalto, P., Hiltunen, V., Hari, P., and Kulmala, M.: Smart-SMEAR: on-line data exploration and visualization tool for SMEAR stations, Boreal Environment Research, 14, 447-457, 2009.

Karvosenoja, N., Kangas, L., Kupiainen, K., Kukkonen, J., Karppinen, A., Sofiev, M., Tainio, M., Paunu, V.-V., Ahtoniemi, P., and Tuomisto, J. T.: Integrated modeling assessments of the population exposure in Finland to primary PM2. 5 from traffic and domestic wood combustion on the resolutions of 1 and 10 km, Air Quality, Atmosphere & Health, 4, 179-188, 2011.

Kittelson, D. B.: Engines and nanoparticles: a review, Journal of Aerosol Science, 29, 575-588, 1998.

Kulmala, M., Vehkamäki, H., Petäjä, T., Dal Maso, M., Lauri, A., Kerminen, V.-M., Birmili, W., and McMurry, P.: Formation and growth rates of ultrafine atmospheric particles: a review of observations, Journal of Aerosol Science, 35, 143-176, 2004.

Kulmala, M., Kontkanen, J., Junninen, H., Lehtipalo, K., Manninen, H. E., Nieminen, T., Petäjä, T., Sipilä, M., Schobesberger, S., and Rantala, P.: Direct observations of atmospheric aerosol nucleation, Science, 339, 943-946, 2013.

Kulmala, M., Luoma, K., Virkkula, A., Petäjä, T., Paasonen, P., Kerminen, V.-M., Nie, W., Qi, X., Shen, Y., and Chi, X.: On the mode-segregated aerosol particle number concentration load: contributions of primary and secondary particles in Hyytiälä and Nanjing, Boreal Environment Research, 21, 319-331, 2016.

Kuusinen, N., Kolari, P., Levula, J., Porcar-Castell, A., Stenberg, P., and Berninger, F.: Seasonal variation in boreal pine forest albedo and effects of canopy snow on forest reflectance, Agricultural and Forest Meteorology, 164, 53-60, 2012.

Lack, D., and Cappa, C.: Impact of brown and clear carbon on light absorption enhancement, single scatter albedo and absorption wavelength dependence of black carbon, Atmospheric Chemistry and Physics, 10, 4207-4220, 2010.

Leskinen, A., Arola, A., Komppula, M., Portin, H., Tiitta, P., Miettinen, P., Romakkaniemi, S., Laaksonen, A., and Lehtinen, K.: Seasonal cycle and source analyses of aerosol optical properties in a semi-urban environment at Puijo station in Eastern Finland, Atmospheric Chemistry and Physics, 12, 5647, 2012.

Li, J., Carlson, B. E., Dubovik, O., and Lacis, A. A.: Recent trends in aerosol optical properties derived from AERONET measurements, Atmospheric Chemistry and Physics, 14, 12271-12289, 2014.

Lihavainen, H., Hyvärinen, A., Asmi, E., Hatakka, J., and Viisanen, Y.: Long-term variability of aerosol optical properties in northern Finland, Boreal Environment Research, 20, 526-541, 2015.

Lohmann, U., and Feichter, J.: Impact of sulfate aerosols on albedo and lifetime of clouds: A sensitivity study with the ECHAM4 GCM, Journal of Geophysical Research: Atmospheres, 102, 13685-13700, 1997.

Muller, T., Henzing, J., De Leeuw, G., Wiedensohler, A., Alastuey, A., Angelov, H., Bizjak, M., Coen, M., Engstrom, J., and Gruening, C.: Characterization and intercomparison of aerosol absorption photometers: result of two intercomparison workshops, Atmospheric Measurement Techniques, 4, 245-268, 2011.

Mätzler, C.: MATLAB functions for Mie scattering and absorption, version 2, Institut für Angewandte Physik, University of Bern, 2002.

Nessler, R., Weingartner, E., and Baltensperger, U.: Effect of humidity on aerosol light absorption and its implications for extinction and the single scattering albedo illustrated for a site in the lower free troposphere, Journal of Aerosol Science, 36, 958-972, 2005.

Pandolfi, M., Alados-Arboledas, L., Alastuey, A., Andrade, M., Angelov, C., Artiñano, B., Backman, J., Baltensperger, U., Bonasoni, P., and Bukowiecki, N.: A European aerosol phenomenology–6: scattering properties of atmospheric aerosol particles from 28 ACTRIS sites, Atmospheric Chemistry and Physics, 18, 7877-7911, 2018.

Saarikoski, S., Makela, T., Hillamo, R., Aalto, P. P., Kerminen, V., and Kulmala, M.: Physico-chemical characterization and mass closure of size-segregated atmospheric aerosols in Hyytiala, Finland, Boreal Environment Research, 10, 385-400, 2005.

Sandradewi, J., Prévôt, A. S., Szidat, S., Perron, N., Alfarra, M. R., Lanz, V. A., Weingartner, E., and Baltensperger, U.: Using aerosol light absorption measurements for the quantitative determination of wood burning and traffic emission contributions to particulate matter, Environmental Science & Technology, 42, 3316-3323, 2008.

Schnaiter, M., Linke, C., Möhler, O., Naumann, K. H., Saathoff, H., Wagner, R., Schurath, U., and Wehner, B.: Absorption amplification of black carbon internally mixed with secondary organic aerosol, Journal of Geophysical Research: Atmospheres, 110, 2005.

Schuster, G. L., Dubovik, O., and Holben, B. N.: Angstrom exponent and bimodal aerosol size distributions, Journal of Geophysical Research: Atmospheres, 111, 2006.

Shen, Y., Virkkula, A., Ding, A., Wang, J., Chi, X., Nie, W., Qi, X., Huang, X., Liu, Q., and Zheng, L.: Aerosol optical properties at SORPES in Nanjing, east China, Atmospheric Chemistry and Physics, 18, 5265-5292, 2018.

Sheridan, P. J., and Ogren, J. A.: Observations of the vertical and regional variability of aerosol optical properties over central and eastern North America, Journal of Geophysical Research: Atmospheres, 104, 16793-16805, 1999.

Sherman, J., Sheridan, P., Ogren, J., Andrews, E., Hageman, D., Schmeisser, L., Jefferson, A., and Sharma, S.: A multi-year study of lower tropospheric aerosol variability and systematic relationships from four North American regions, Atmospheric Chemistry and Physics, 15, 12487-12517, 2015.

Tunved, P., Hansson, H.-C., Kerminen, V.-M., Ström, J., Dal Maso, M., Lihavainen, H., Viisanen, Y., Aalto, P., Komppula, M., and Kulmala, M.: High natural aerosol loading over boreal forests, Science, 312, 261-263, 2006.

Twomey, S.: Aerosols, clouds and radiation, Atmospheric Environment, 25A, 2435-2442, 1991.

Tørseth, K., Aas, W., Breivik, K., Fjæraa, A. M., Fiebig, M., Hjellbrekke, A.-G., Lund Myhre, C., Solberg, S., and Yttri, K. E. J. A. C.: Introduction to the European Monitoring and Evaluation Programme (EMEP) and observed atmospheric composition change during 1972–2009, Atmospheric Chemistry and Physics, 12, 5447-5481, 2012.

Warren, S. G., and Wiscombe, W. J. J. J. o. t. A. S.: A model for the spectral albedo of snow. II: Snow containing atmospheric aerosols, 37, 2734-2745, 1980.

Virkkula, A., Backman, J., Aalto, P., Hulkkonen, M., Riuttanen, L., Nieminen, T., Dal Maso, M., Sogacheva, L., De Leeuw, G., and Kulmala, M.: Seasonal cycle, size dependencies, and source analyses of aerosol optical properties at the SMEAR II measurement station in Hyytiala, Finland, Atmospheric Chemistry and Physics, 11, 4445, 2011.

WMO/GAW: Aerosol Measurement Procedures, Guidelines and Recommendations, GAW Report No. 153, World Meteorological Organization, Geneva, Switzerland, 2003.

WMO/GAW: Aerosol Measurement Procedures, Guidelines and Recommendations, 2nd edition, GAW Report No. 227, World Meteorological Organization, Geneva, Switzerland, 2016.

Zhang, R., Khalizov, A. F., Pagels, J., Zhang, D., Xue, H., and McMurry, P. H.: Variability in morphology, hygroscopicity, and optical properties of soot aerosols during atmospheric processing, Proceedings of the National Academy of Sciences, 105, 10291-10296, 2008.

Zieger, P., Aalto, P., Aaltonen, V., Äijälä, M., Backman, J., Hong, J., Komppula, M., Krejci, R., Laborde, M., and Lampilahti, J.: Low hygroscopic scattering enhancement of boreal aerosol and the implications for a columnar optical closure study, Atmospheric Chemistry and Physics, 15, 7247-7267, 2015.

Zotter, P., Herich, H., Gysel, M., El-Haddad, I., Zhang, Y., Močnik, G., Hüglin, C., Baltensperger, U., Szidat, S., and Prévôt, A. S.: Evaluation of the absorption Ångström exponents for traffic and wood burning in the Aethalometer-based source apportionment using radiocarbon measurements of ambient aerosol, Atmospheric Chemistry and Physics, 17, 4229-4249, 2017.

Ångström, A.: On the atmospheric transmission of sun radiation and on dust in the air, Geografiska Annaler, 11, 156-166, 1929.

Table 1: Average values of the AOPs for the PM10 particles. The average values were calculated from all valid data.

PM10	λ (nm)	mean ± SD	1 %	10 %	25 %	50 %	75 %	90 %	99 %
σ_{sca} (Mm^{-1})	450	21.8 ± 23.3	1.8	4.5	7.6	14.2	26.8	48.5	114.1
	550	15.2 ± 16.7	1.3	3.4	5.5	9.8	18.3	33.4	82.5
	700	9.5 ± 10.5	0.8	2.3	3.7	6.3	11.3	20.3	52.3
σ_{bsca} (Mm^{-1})	450	2.5 ± 2.9	0.2	0.6	1.0	1.8	3.2	5.3	11.1
	550	2.0 ± 1.8	0.2	0.5	0.8	1.4	2.5	4.2	8.8
	700	1.6 ± 1.5	0.2	0.4	0.7	1.2	2.0	3.4	7.4
σ_{abs} (Mm^{-1})	370	3.0 ± 3.6	0.2	0.6	1.0	1.9	3.6	6.6	18.1
	470	2.5 ± 2.9	0.2	0.5	0.8	1.6	3.0	5.4	14.3
	520	2.2 ± 2.4	0.1	0.4	0.7	1.4	2.6	4.7	12.3
	590	1.9 ± 2.2	0.1	0.4	0.7	1.3	2.4	4.2	10.8
	660	1.8 ± 2.0	0.1	0.3	0.6	1.2	2.2	3.8	9.9
	880	1.3 ± 1.4	0.1	0.3	0.5	0.9	1.6	2.9	7.2
	950	1.2 ± 1.3	0.1	0.3	0.4	0.8	1.5	2.6	6.5
ω_0	450	0.88 ± 0.07	0.64	0.80	0.85	0.89	0.93	0.95	0.98
	550	0.87 ± 0.07	0.62	0.78	0.84	0.88	0.92	0.94	0.98
	700	0.84 ± 0.08	0.55	0.74	0.80	0.85	0.90	0.93	0.97
b	450	0.13 ± 0.03	0.08	0.10	0.11	0.12	0.14	0.16	0.21
	550	0.14 ± 0.03	0.09	0.11	0.13	0.14	0.16	0.17	0.21
	700	0.19 ± 0.07	0.07	0.13	0.15	0.18	0.21	0.25	0.44
α_{sca}	450/550	1.73 ± 0.52	0.23	1.03	1.49	1.82	2.09	2.29	2.58
	450/700	1.80 ± 0.55	0.32	1.00	1.53	1.88	2.17	2.39	2.80
	550/700	1.85 ± 0.64	0.23	0.95	1.53	1.95	2.26	2.50	3.15
α_{abs}	370/520	0.95 ± 0. 48	-0.29	0.51	0.76	0.98	1.16	1.32	1.97
	370/950	0.95 ± 0.36	-0.16	0.55	0.80	0.99	1.13	1.24	1.69
	470/660	0.95 ± 0.49	-0.52	0.52	0.80	1.01	1.15	1.29	2.07
	470/950	0.99 ± 0.41	-0.32	0.58	0.86	1.06	1.18	1.28	1.83
	660/950	1.02 ± 0.57	-0.77	0.57	0.90	1.11	1.23	1.34	2.17
n	450	1.541 ± 0.065	1.330	1.478	1.512	1.542	1.572	1.607	1.697
	550	1.518 ± 0.067	1.289	1.452	1.490	1.522	1.550	1.581	1.674
	700	1.491 ± 0.091	1.247	1.379	1.454	1.501	1.536	1.574	1.740
k	450	0.021 ± 0.020	0.002	0.006	0.009	0.016	0.026	0.039	0.097
	550	0.020 ± 0.018	0.002	0.006	0.010	0.016	0.025	0.038	0.089
	700	0.022 ± 0.019	0.003	0.007	0.011	0.018	0.027	0.041	0.092
$RFE_{H\&S}$ (Wm^{-2})	550	-22 ± 6	-32	-28	-26	-23	-19	-16	-3
RFE_{S} (Wm^{-2})	550	-35 ± 32	-97	-82	-67	-26	-5	0	12
$RFE_{S,moist}$ (Wm^{-2})	550	-32 ± 28	-85	-72	-60	-24	-5	-2	5

Table 2: Average values of the AOPs for the PM1 particles. The average values were calculated from all valid data; th~~us~~erefore if compared with the PM10 average values, there is a 4-year shorter dataset.

PM1	λ (nm)	mean ± SD	1 %	10 %	25 %	50 %	75 %	90 %	99 %
σ_{sca} (Mm^{-1})	450	17.7 ± 19.2	1.2	3.1	5.6	11.3	22.3	40.4	96.1
	550	11.4 ± 13.0	0.8	2.1	3.6	7.1	14.1	26.1	64.8
	700	6.3 ± 7.5	0.4	1.2	2.0	3.8	7.6	14.4	37.4
σ_{bsca} (Mm^{-1})	450	2.1 ± 2.0	0.2	0.4	0.8	1.4	2.7	4.5	9.7
	550	1.6 ± 1.5	0.1	0.3	0.6	1.1	2.0	3.4	7.5
	700	1.2 ± 1.2	0.1	0.3	0.5	0.8	1.5	2.6	5.9
σ_{abs} (Mm^{-1})	370	2.4 ± 2.9	0.1	0.4	0.8	1.6	2.9	5.2	15.0
	470	2.0 ± 2.3	0.1	0.4	0.7	1.3	2.4	4.3	11.7
	520	1.7 ± 1.9	0.1	0.3	0.6	1.2	2.1	3.7	10.0
	590	1.6 ± 1.7	0.1	0.3	0.5	1.0	1.9	3.3	8.8
	660	1.4 ± 1.6	0.1	0.3	0.5	01.0	1.8	3.1	8.0
	880	1.1 ± 1.1	0.1	0.2	0.4	0.7	1.3	2.3	5.8
	950	0.9 ± 1.0	0.0	0.2	0.3	0.6	1.2	2.0	5.1
ω_0	450	0.88 ± 0.08	0.62	0.78	0.84	0.89	0.93	0.96	0.98
	550	0.85 ± 0.08	0.59	0.75	0.81	0.87	0.91	0.94	0.98
	700	0.80 ± 0.10	0.48	0.67	0.75	0.81	0.87	0.91	0.96
b	450	0.13 ± 0.03	0.07	0.10	0.11	0.13	0.14	0.17	0.23
	550	0.15 ± 0.03	0.09	0.12	0.13	0.15	0.17	0.19	0.24
	700	0.23 ± 0.13	-0.06	0.14	0.17	0.21	0.26	0.34	0.78
α_{sca}	450/700	2.22 ± 0.44	0.88	1.70	1.99	2.28	2.51	2.66	2.95
	450/550	2.36 ± 0.55	0.74	1.76	2.09	2.41	2.66	2.87	3.70
	550/700	2.48 ± 0.81	0.25	1.73	2.16	2.52	2.82	3.13	4.69
α_{abs}	370/520	0.96 ± 0.61	-0.67	0.47	0.74	0.99	1.20	1.39	2.32
	370/950	0.97 ± 0.44	-0.36	0.52	0.80	1.03	1.19	1.33	1.96
	470/660	0.94 ± 0.66	-0.94	0.46	0.76	1.00	1.17	1.33	2.35
	470/950	1.03 ± 0.51	-0.51	0.56	0.87	1.11	1.25	1.39	2.24
	660/950	1.13 ± 0.72	-1.10	0.60	0.97	1.20	1.35	1.54	2.96
n	450	1.509 ± 0.057	1.348	1.441	1.478	1.513	1.542	1.568	1.634
	550	1.484 ± 0.054	1.338	1.422	1.456	1.487	1.516	1.540	1.598
	700	1.471 ± 0.074	1.294	1.393	1.435	1.472	1.505	1.537	1.677
k	450	0.025 ± 0.020	0.003	0.008	0.013	0.020	0.031	0.045	0.099
	550	0.025 ± 0.018	0.004	0.009	0.014	0.021	0.031	0.044	0.093
	700	0.028 ± 0.019	0.005	0.011	0.017	0.024	0.035	0.049	0.098

Table 3: Slopes of the trends (in absolute values and in estimated percentages per year) and their statistical significance. The lower and upper limits in the 95 % confidence interval for different optical properties are also shown. The trend in the percentage was determined by comparing the slope of the trend with the overall median of the data.

		PM10					PM1				
	λ (nm)	Trend (yr^{-1})		Lower (yr^{-1})	Upper (yr^{-1})	*p*-value	Trend (yr^{-1})		Lower (yr^{-1})	Upper (yr^{-1})	*p*-value
σ_{sca} (Mm^{-1})	550	-0.32	-3 %	-0.52	-0.17	< 0.01	-0.30	-4 %	-0.55	-0.12	< 0.01
σ_{bsca} (Mm^{-1})	550	-0.038	-3 %	-0.070	-0.021	< 0.01	-0.051	-5 %	-0.087	-0.013	< 0.01
σ_{abs} (Mm^{-1})	520	-0.086	-6 %	-0.133	-0.044	< 0.01	-0.141	-12 %	-0.166	-0.098	< 0.01
ω_0	550	2.2e-3	0.3 %	0.7e-3	3.6e-3	< 0.01	5.5e-3	0.6 %	1.5e-3	10e-3	< 0.01
b	550	1.3e-3	0.9 %	0.9e-3	1.7e-3	< 0.01	1.5e-3	1 %	0.7e-3	2.6e-3	< 0.01
α_{sca}	450/700	0.012	0.7 %	-0.001	0.024	0.07	0.014	0.6 %	0.004	0.024	< 0.01
α_{abs}	370/950	-1.5e-4	0 %	-3.0e-3	2.9e-5	0.95	-3.5e-3	-0.3 %	-7.9e-3	13e-3	0.34
n	550	-2.0e-3	-0 %	-3.8e-3	0.6e-3	0.11	-5.7e-3	-0.4 %	-7.5e-3	-2.9e-3	< 0.01
k	550	-6.6e-4	-4 %	-9.1e-4	-3.8e-4	< 0.01	-1.3e-3	-6 %	-2.0e-3	-0.7e-3	< 0.01
$RFE_{H\&S}$ (Wm^{-2})	550	-0.30	-1 %	-0.43	-0.20	< 0.01					
RFE_{S} (Wm^{-2})	550	-0.43	-2 %	-0.64	-0.25	< 0.01					
$RFE_{S,moist}$ (Wm^{-2})	550	-0.39	-2 %	-0.50	-24	< 0.01					
N_{tot} (cm^{-3})		-40	-3 %	-52	-28	< 0.01					
V_{tot} (µg cm^{-3})		-0.093	-4 %	-0.120	-0.064	< 0.01					
VMD_{tot} (nm)		-12	-1 %	-17	-7	< 0.01					

Table 4: Slopes of the seasonal trends and their statistical significance for σ_{sca} and σ_{abs}. The trend in the percentage was determined by comparing the slope of the trend with the seasonal median of the data.

	σ_{sca} (Mm^{-1})					σ_{abs} (Mm^{-1})				
	Trend (yr^{-1})		Lower (yr^{-1})	Upper (yr^{-1})	*p*-value	Trend (yr^{-1})		Lower (yr^{-1})	Upper (yr^{-1})	*p*-value
Spring	-0.44	-5 %	-0.84	-0.04	< 0.05	-0.12	-9 %	-0.20	-0.05	< 0.01
Summer	-0.38	-3 %	-0.79	-0.14	< 0.01	-0.06	-5 %	-0.11	-0.03	< 0.01
Autumn	-0.12	-1 %	-0.49	0.17	0.48	-0.04	-3 %	-0.10	0.03	0.14
Winter	-0.85	-7 %	-1.60	-0.20	< 0.01	-0.17	-8 %	-0.31	-0.03	< 0.05

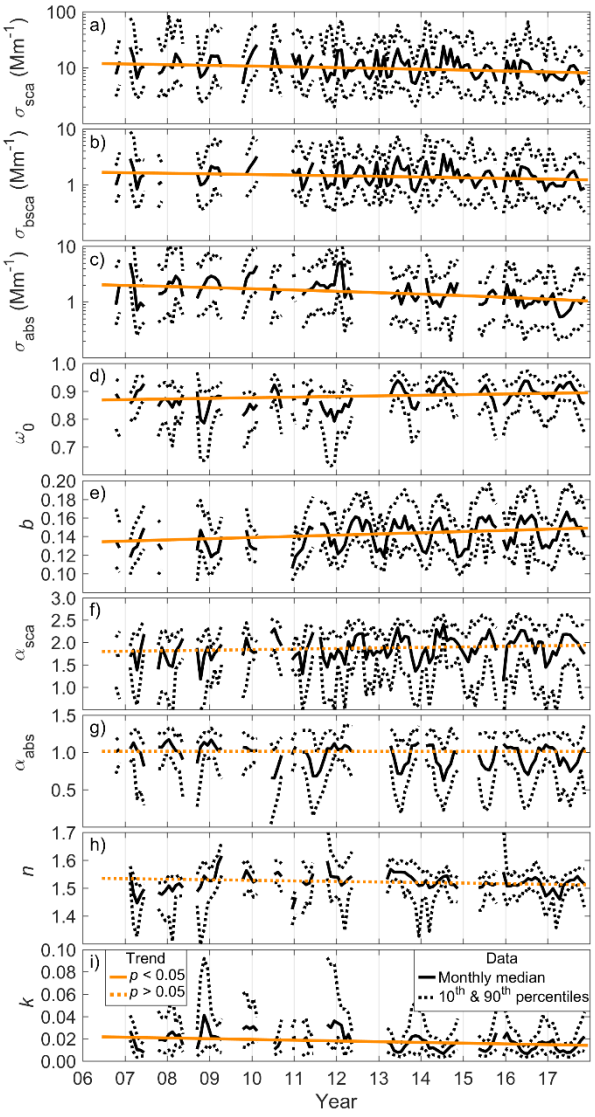

Figure 1: Time series of the AOPs. The uniform black line presents the monthly median and the dotted black lines present the monthly 10th and 90th percentiles. The trends (see Table 3) of the AOPs are shown with orange lines. If the trend was statistically significant, the line is uniform and if the *p*-value of the trend was > 0.05, the line is dashed.

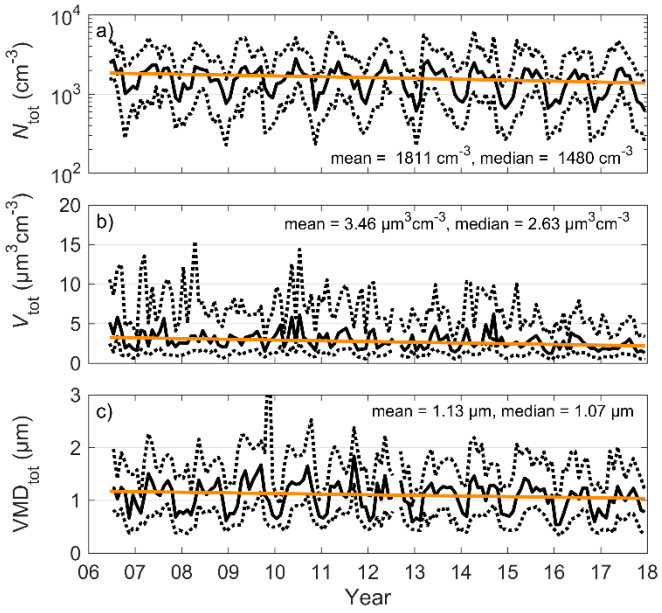

Figure 2: Time series and trends of the total particle (D_p < 10 µm) a) number concentration (N_{tot}), b) volume (V_{tot}) and c) VMD_{tot}. The mean and median values of the variables are also marked in the subfigures and the statistics of their slopes are presented in Table 3. The explanations for the different lines are the same as in Fig. 1 ~~Fig. 1~~.

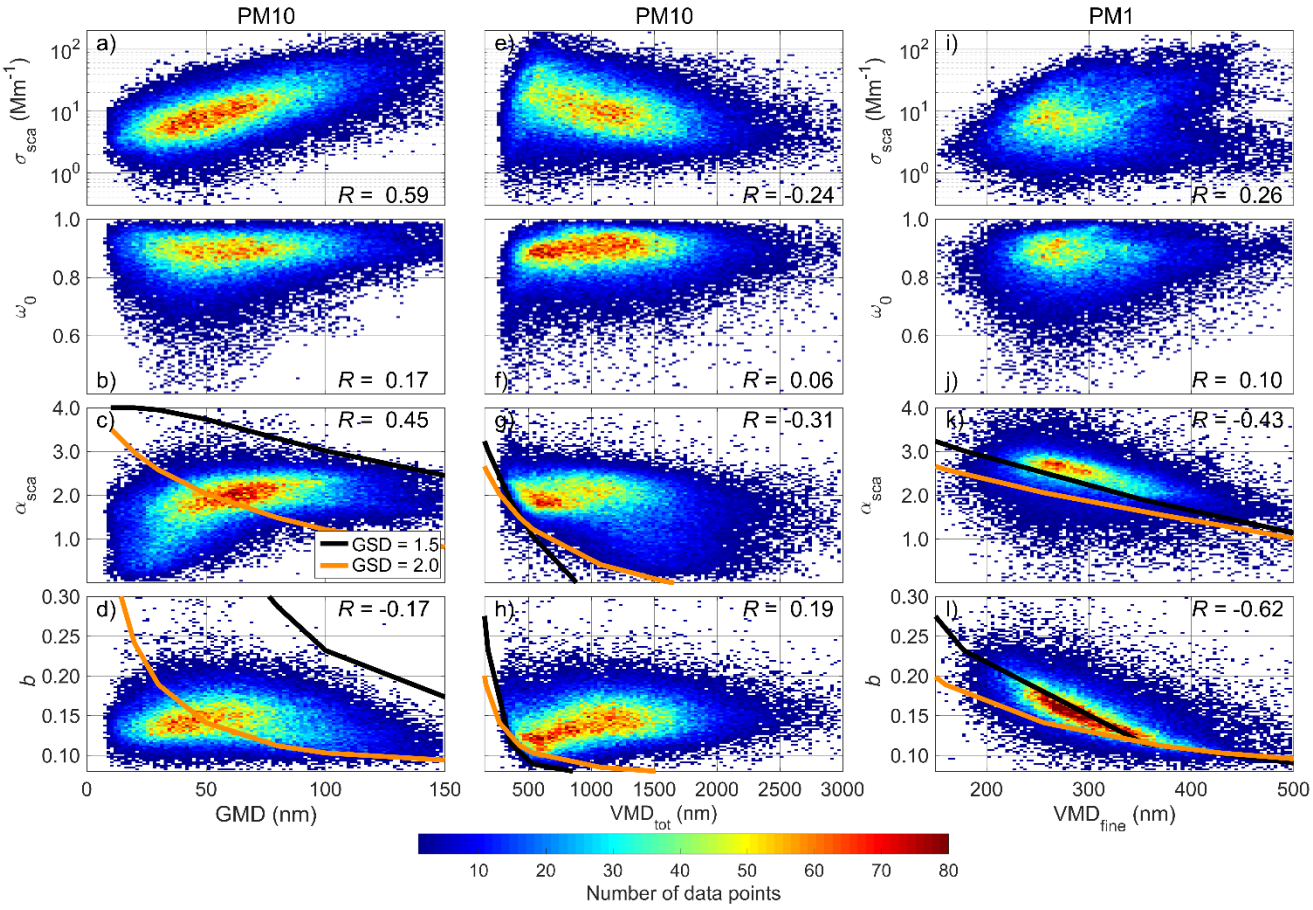

Figure 3: Relationships between the various AOPs, GMD and VMD. Subplots a) – d) describe the correlation between the PM10 AOPs and GMD; subplots e) – h) describe the correlation between the PM10 AOPs and VMD_{tot}; and the subplots i) – l) describe the correlation between the PM1 AOPs and VMD_{fine}. The correlation coefficients of the linear regressions are given in each subfigure. The color-coding represents the number of data points in a grid point. In each subfigure, there are 100 grid points on both axes, making 10 000 grid points in total. The orange and black lines represent the values calculated from the unimodal size distributions, which were generated for different GMDs with geometric standard deviation GSD = 2.0 and 1.5 nm. The scattering was modeled from the generated size distribution at wavelengths 450, 550, and 700 nm with a refractive index *m* = 1.517 + 0.19i.

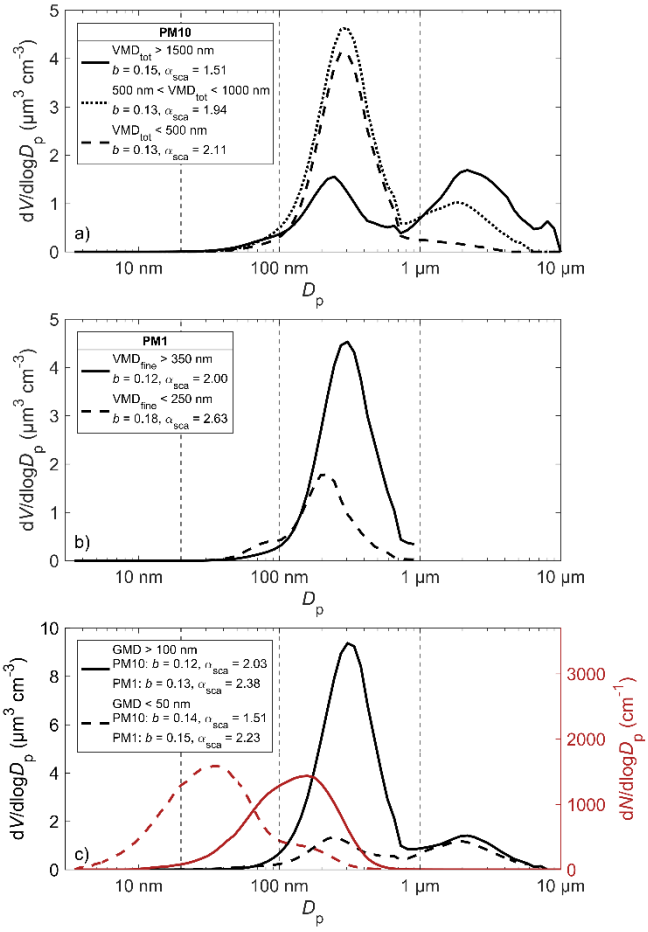

Figure 4: Median volume and number size distributions for the various VMD and GMD limits. The median *b* and α_{sca} for the VMD and GMD limits are given in each legend box. The vertical grid lines represent the typical diameter limits for the nucleation, Aitken, accumulation and coarse particle modes (same as in Figs. S4 and S6 ~~Fig. 3~~). a) Volume size distribution for different PM10 VMD_{tot} limits. b) Volume size distribution for different PM1 VMD_{fine} limits. c) Volume and number size distribution for different PM10 and GMD limits. The c) subfigure also represents volume and number size distribution for different PM1 and GMD limits as well, since the GMD is practically the same for PM10 and PM1 particles.

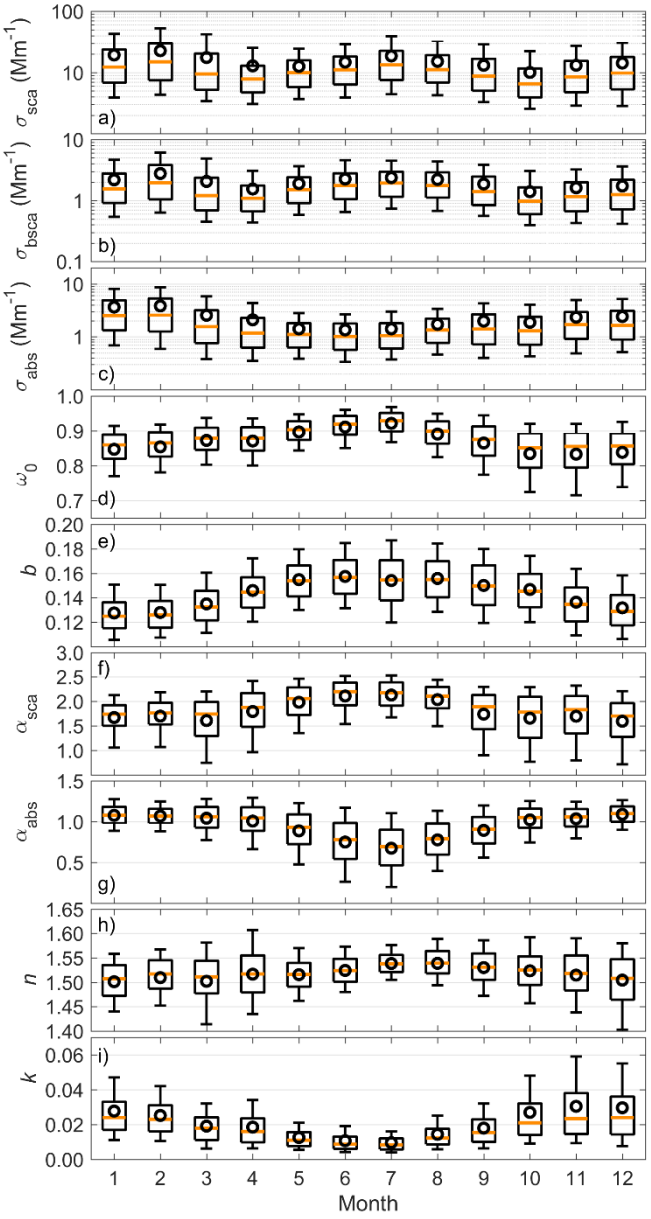

Figure 5: Seasonal variation in the aerosol optical properties for PM10 particles. The boxes represent the 25th and 75th percentiles and the whiskers the 10th and 90th percentiles of the data. The orange line is the median and the mean is presented with a black circle.

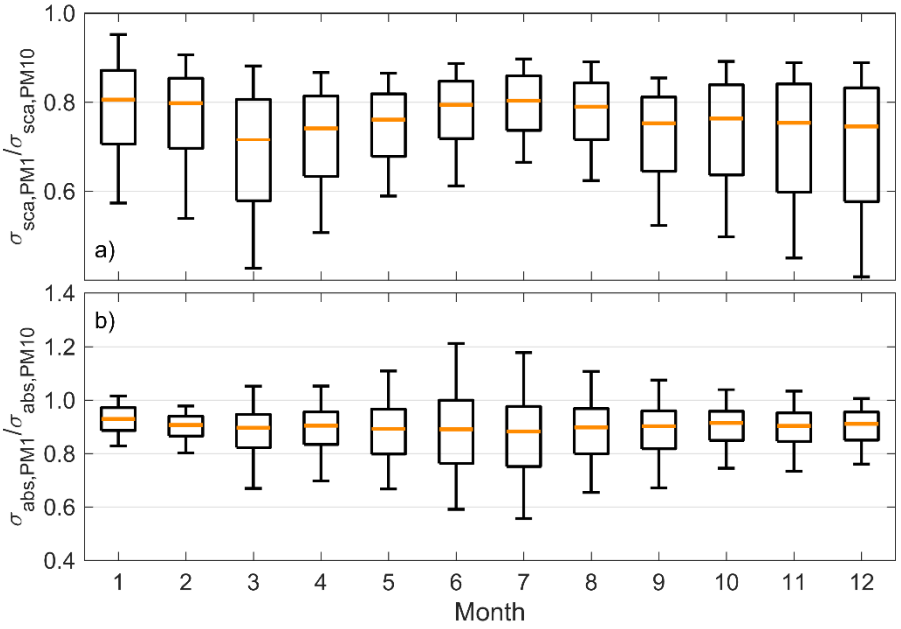

Figure 6: Seasonal variation in the PM1/PM10 ratio for a) σ_{sca} and b) σ_{abs}. The explanation for the boxplots are the same as in Fig. 5.

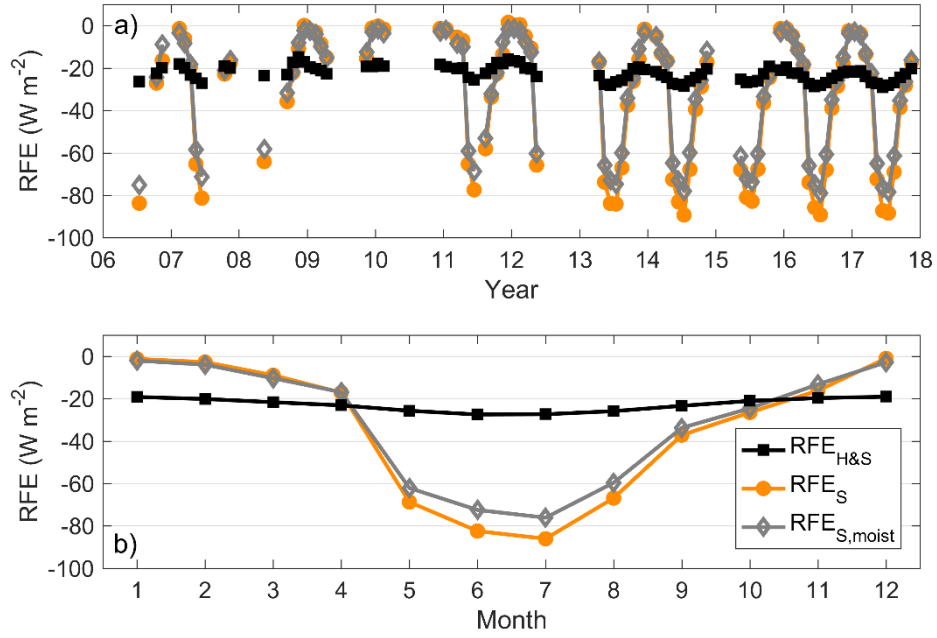

Figure 7: Variations in the different radiative forcing efficiencies at SMEAR II in 2006 – 2018. a) Time series of the $RFE_{H\&S}$, RFE_S, and $RFE_{S,moist}$. The monthly medians are presented if the month had at least 14 days of valid data. b) Seasonal variation of the $RFE_{H\&S}$, RFE_S, and $RFE_{S,moist}$ as overall monthly medians.

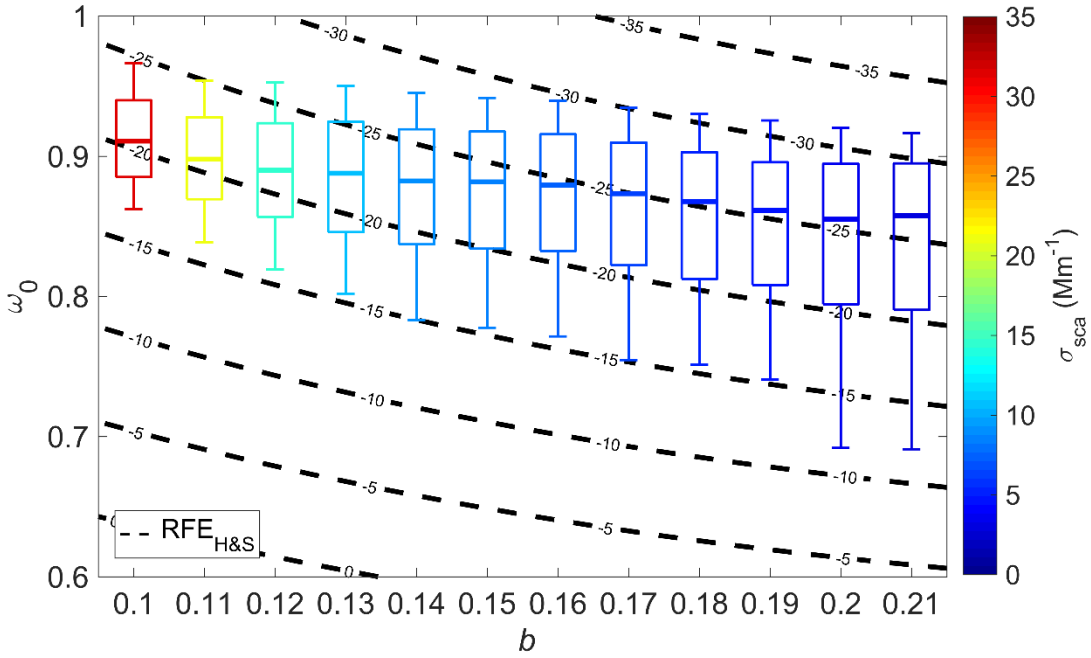

Figure 8: Relationships between ω_0, b and $RFE_{H\&S}$. The $RFE_{H\&S}$ is shown as the dashed isolines in the background. The boxes represent the data measured at SMEAR II and they are colored by the median σ_{sca}. The explanation for the boxplots is the same as in Fig. 5.